LOW DELTA-T SYNDROME DIAGNOSIS AND CORRECTION FOR CHILLED WATER PLANTS

A Thesis

by

AGNES D ALMEIDA

Submitted to the Office of Graduate and Professional Studies of
Texas A&M University
in partial fulfillment of the requirements for the degree of

MASTER OF SCIENCE

Chair of Committee,	David Claridge
Co-Chair of Committee,	Michael Pate
Committee Member,	Juan-Carlos Baltazar
Head of Department,	Andreas Polycarpou

December 2014

Major Subject: Mechanical Engineering

ABSTRACT

This thesis presents a study of the low delta-T syndrome in the DFW Airport. The chilled water system was modeled separately to understand its behavior and identify the possible causes for the low delta-T. The aim of this study is to propose energy saving measures that would improve the plant's overall efficiency.

Data for the chillers and the chilled water storage tank was analyzed to determine the DFW Airport's chilled water plant operation. The chiller simulation, following Gordon and Ng's model, provided the starting point to the optimization process. The chiller model's input variables were chilled water leaving temperature, condenser water entering temperature and water flow.

A detailed study of the TES tank was made to ensure that the proposed changes would enable the TES tank to provide cooling for the airport, particularly during the summer months from June through September from 3 pm to 6 pm when the chillers are turned off due to the rate structure.

The chilled water leaving temperatures were set to provide enough chilled water to meet the cooling loads and provide the necessary chilled water to fill the TES tank. The other variables, namely condenser water leaving temperature and water flow, do not affect the rate at which the tank is filled. Thus, the values obtained through the optimization process are maintained.

The proposed reset schedule for the DFW Airport is the following: constant condenser water flow of 100,000 ft^3/hr (~12,500 gpm), an approach temperature of 5˚F

whenever the outside air wet bulb temperature is above 55˚F, otherwise maintain a 60˚F condenser supply temperature. The reset schedule proposed for the chilled water supply temperature is 37˚F from March through September and 42˚F from October through December, January and February.

The chiller simulation and the secondary pumps simulation were used to determine the power required to run the system under the proposed reset schedules. Initially, the condenser water flow rate was set to current operation because it was not possible to predict the additional power required by the condenser pumps. A condenser pumping power model was not built due to lack of data. The total energy savings predicted were 1,589,000 kWh, which represents 3.8% savings. Finally, the simulation was run using the proposed condenser water flow rate of 100,000 ft^3/hr (~12,465 gpm) per working chiller, year round. The predicted energy savings were 3,237,000 kWh, which represents 7.7% savings. However, the savings will be less than 7.7% when the additional power required by the condenser pumps is considered.

DEDICATION

To my family

ACKNOWLEDGEMENTS

I would like to sincerely thank my committee chair, Dr. David Claridge, for guiding me every step of the way during my thesis. I would also like to thank the committee members, Dr. Juan-Carlos Baltazar and Dr. Michael Pate, for their input throughout this process.

I would also like to thank Joseph Martinez whose support and advice got me through my time in ESL. I would also like to thank Ahmet Ugursal for his help and especially Donny Lumpkin and the DFW Airport staff for being so helpful with providing data and answering questions I had along the way.

Thank you to my friends and colleagues, especially my office mates, Mitch Paulus and Alaina Jones, for being so cooperative and supportive, and for making my time in ESL more enjoyable. Also, thank you to Hala Nemer for being an invaluable help in completing this thesis.

I wish to thank the Energy Systems Laboratory and the Mechanical Engineering department members, faculty and staff for making my time at Texas A&M University a great experience. Most importantly, I would like to thank my family for the love, encouragement and support.

I could not have done this without the help and support of all of you. Thank you.

NOMENCLATURE

DFW	Dallas Fort Worth
OM	On-site manufactured
TES	Thermal Energy Storage
AHU	Air Handling Units
CUP	Central Utility Plant
ChW	Chilled water
CW	Condenser water
T	Temperature
s	Entropy
COP	Coefficient of performance
ΔE	Change of internal energy over one cycle
ΔS	Change of entropy over one cycle
Q_{cond}	Heat exchanged in the condenser
Q_{cond}^{leak}	Heat leak at the condenser
Q_{evap}	Heat exchanged in the evaporator
Q_{evap}^{leak}	Heat leak at the evaporator
P_{in}	Input power
Q_{comp}^{leak}	Heat leak at the compressor
ΔS_{int}	Rate of internal entropy production
Q_{eqv}^{leak}	Irreversibilities due to heat leaks and,

R	Irreversibilities due to finite rate heat exchange
V_{cond}	Water flow going through the condenser
T_{cond}^{in}	Water temperature entering the condenser
T_{cond}^{out}	Water temperature leaving the condenser
T_{evap}^{out}	Water temperature leaving the evaporator
T_{evap}^{in}	Water temperature entering the evaporator
$ChWST$	Chilled Water supply temperature
Twb	Outside air wet bulb temperature
$x_{ChWtank}$	Chilled water ratio in the tank
V_{ChW}	Tank chilled water volume
V_{total}	Tank total volume capacity
${x_{ChWtank}}^{-1}$	Tank chilled water ratio from the previous time stamp
$\dot{V}_{ChW}$	Volumetric flow rate of chilled water in and out of the tank
t	Time period over which the tank volumetric flow rate is measured
$\dot{m}$	Mass flowrate
C_p	Specific heat capacity
OAT	Outside air temperature

TABLE OF CONTENTS

Page

LIST OF FIGURES

Page

CHAPTER I

INTRODUCTION

Background and problem statement

Chilled water plants are widely used to provide building cooling and account for a significant part of a facility's energy consumption. Since chillers consume the majority of the energy used by chilled water plants, it is important to ensure efficient chiller operation.

When analyzing plant and chiller performance, an important factor to consider is the temperature difference between the return and supply chilled water. This temperature difference will be referred to as delta-T. When this delta-T drops well below design level for certain conditions, this occurrence is known as low delta-T syndrome. Low delta-T syndrome affects numerous facilities and usually takes place when cooling loads are low. However, there are several causes for low delta-T syndrome that will be discussed and analyzed in detail during this study. It is important to minimize or avoid low delta-T in chillers and plants because efficiency drops and energy is squandered by increasing chiller energy usage and pumping power.

Specifically, this thesis focuses on the Dallas Fort Worth (DFW) Airport chilled water plant. This plant functions as a primary- secondary system and is comprised of 6 on-site manufactured (OM) 5,500 ton centrifugal chillers, a 90,000 ton-hr Thermal Energy Storage (TES) tank, six 150 hp constant speed primary pumps and four 450 hp variable speed secondary pumps. This chilled water plant provides cooling for 5

terminals, each of these terminals having north and south stations. It also provides cooling for a business center, a hotel and various other buildings. In total, the DFW Airport's maximum cooling load is about 170,000 kBtu/hr. In the DFW Airport's chilled water plant delta-T is in the 15˚F- 20˚F delta-T range. However, delta-T drops below 15˚F as loads get lower, dropping significantly when loads are lower than 70,000 kBtu/hr. This delta-T drop represents an unwanted increase in energy usage and operation cost for the plant. Thus, the goal of this study is to identify the possible causes for the low delta-T and optimize those variables to reduce energy consumption and improve the plant performance.

Objectives

The objective of this study is to investigate the causes for the low delta-T affecting the DFW Airport. Since there are tens of buildings and hundreds of AHUs in this facility, the study will be carried out on the water side of the chilled water system at plant level. The main objective is to identify the measures that would improve the plant delta-T and therefore improve the plant efficiency.

In order to identify measures that improve the plant's delta-T, the following tasks were completed in this study:

1. Analyze plant and chillers performance in the interest of identifying possible causes for the low delta-T syndrome.
2. Determine the variables that are plant-controlled and subject to optimization.
3. Build a system model to simulate plant performance and predict plant behavior under new conditions.

4. Find by optimization, the cost-effective measures that can be applied to the Central Utility Plant (CUP) in the DFW Airport.

CHAPTER II

LITERATURE REVIEW

Low Delta-T syndrome

Low delta-T syndrome occurs when the temperature difference between the supply and return chilled water is lower than designed. The low delta-T syndrome usually occurs when cooling loads drop and is found in almost every Central Plant. Problems such as higher pump energy usage, higher chiller energy usage or failure to meet cooling loads are direct consequences of low delta-T syndrome.

There are two basic chiller start/stop control strategies: one based on system flow rate and the other based on load. The two strategies should be effectively the same since flow depends on load in a variable flow system. However, when load and flow do not track, and when low delta-T occurs neither strategy works ideally.

The flow-based strategies stage chillers and primary chilled water pumps to keep the primary flow larger than the secondary flow. This staging helps avoid the mixing of supply chilled water and return chilled water to meet flow requirements. In this case, the secondary supply water temperature is equal to the primary water temperature leaving the chillers. Another primary pump and chiller start when flow in the secondary loop exceeds that of the primary loop. Similarly, both chiller and primary pump shut off when the flow in the secondary loop exceeds that of the primary loop by the flow of one pump.

The load-based strategy measures either system load directly or uses indirect indications of load like return water temperature. When the working chillers are

operating at their maximum capacity, a new chiller is turned on. When the measured load is less than the operating capacity of the operating chillers by one chiller, a chiller is stopped.

In addition to the mixing of return water with supply water, a variety of reasons can cause a drop in the delta-T. These reasons can be divided into three categories: causes that can be avoided, causes that cannot be avoided and causes that can be resolved but may not result in energy savings.

Avoidable causes for the drop of delta-T include improper setpoints and control calibrations, use of three way valves, improper coil selection, improperly selected control valves, improperly piped coils, improper tertiary connection and control, and uncontrolled process loads. Causes that can be resolved but do not result in energy savings include laminar flow and chilled water reset. Finally, the causes that cannot be avoided are: reduced coil effectiveness, outdoor air economizers and 100% outside air systems. (Taylor 2002)

A high delta-T is cost effective and therefore desirable for a central plant operation. The chilled water supply water temperature relies on central plant operation while the chilled water return temperature mainly depends on cooling coil performance of air handling units (AHU). Many factors affect the AHU cooling coil performance, such as cooling coil size, chilled water supply temperature, AHU supply air temperature, space cooling load, outside airflow and conditions, cooling coil fouling conditions and cooling coil control valve types. For instance, the smaller the cooling coil size, the greater the chilled water flow required to maintain the same supply air temperature. In

addition, the chilled water return temperature decreases because of the chilled water flow increase. Cooling coil performance will also change with the chilled water supply temperature. The higher the chilled water supply temperature, the higher the chilled water flow and the lower the chilled water return temperature.

Lower supply air temperatures will require a higher chilled water flow and consequently will result in lower chilled water return temperature. This temperature will also decline for low space cooling loads, high air intake ratio and with the use of 3-way valves. The use of 3-way valves may be the main cause for low chilled water return temperature in some systems rather than partial cooling loads, especially if the cooling coil is designed, operated and maintained properly. It is important to maintain the cooling coil conditions since dirty coils will require extra chilled water flow to maintain the supply air temperature setpoint resulting in lower chilled water return temperatures. (Wang, Zheng et al. 2006)

Since in many systems the root of the low delta-T is located at the coil side, it is important to consider all the important factors that may contribute to this problem. The cooling coil geometric configuration is the inherent factor determining the coil delta-T characteristics. The airside and waterside conditions are extrinsic factors that determine the coil delta-T. In order to study the coil impact on the water to air heat transfer, Zhang, Li and Liu (2012) developed an effectiveness-NTU model used to simulate the cooling coil performance. The effectiveness-NTU coil model with a combined waterside convection coefficient is used to model the coil chilled water leaving temperature at any given airside and waterside conditions. For that particular coil, they conclude that

different waterside correlations generate widely different delta-T prediction results, especially in the laminar region. With variant geometric configurations, the coil delta-T at full load may be higher, equal or lower to that at part load. Coils with more rows, smaller tube diameter, more feeds per row, wider fin spacing and thicker fins will generate higher delta-T. (Zhang, Li et al. 2012)

Unfortunately, systems often have coil related issues such as inadequate coil control valves, incorrect thermostat setpoints and dirty coils. For these systems, flow can be an unreliable indication of load, making plants with chillers that are staged using a system flow-based strategy inefficient. These plants often operate several chillers partially loaded, as opposed to fewer chillers fully or close to fully loaded, which makes for inefficient operation. Minimizing the number of chillers on-line reduces the plant kW/ton since the unneeded pumps and auxiliary devices are also off-line.

For these plants, the best way to stage chillers is using the load-based strategy. Chillers are staged on based on a temperature sensor in the secondary loop chilled water supply. The secondary loop supply chilled water temperature setpoint is set low enough to satisfy the cooling loads. Chillers are staged off based on a temperature sensor in the secondary loop chilled water return. This temperature is an indirect measurement of cooling load, since loads can be calculated by multiplying the flow by the difference in supply and return temperatures. When the load decreases below the capacity of an online chiller, that chiller and pump are staged off. The use of a check valve, which is actually a one-way valve, in the bypass line is advised to prevent return water from mixing with supply water (Avery 2001).The only disadvantage to having a check valve is that the

secondary pumps will be deadheaded if the primary pumps are off and chiller isolation valves are closed. This problem can be avoided simply by shutting off the secondary pumps whenever primary pumps are off. (Taylor 2002)

Gao, Wang and Sun (2011) propose an alternative solution to the deficit flow, which causes mixing of the return water with supply water and results in higher temperature of the chilled water supplied to the AHUs. They suggest a control strategy for secondary pumps that not only eliminates the deficit problem but also enhances the energy efficiency of the chilled water distribution systems. The control strategy provides a method based on a flow limiting technique that can ensure the flow rate in the bypass line is positive. This strategy would also maintain the lowest pump head possible while still satisfying the cooling demands of the AHUs.

The control strategy proposed by Gao, Wang and Sun (2011) uses feedback control, that is to say, it uses the measured water flow rate in the bypass line and compares it to a setpoint value, which is set to be a small positive flow, to rescale the differential pressure setpoint at the main supply. The differential pressure setpoint is compared to the measured differential pressure at the most remote point and generates a control signal. The control signal is rescaled to generate an optimal setpoint of the differential pressure at supply for the secondary pump control. This way the chilled water flow is the minimum necessary to maintain the required differential pressure. (Gao 2011)

Chiller modeling

Several energy efficiency measures have been studied for central chilled water plants since they are a significant part of energy consumption in buildings. The measures that are most commonly used are the following: chilled water supply temperature reset, cooling tower approach temperature reset, secondary loop differential pressure, and condenser water flow rate. Chiller models are used to predict the effect of these measures in chilled water plants.

Chiller plant models are either component-based or system-based. The component-based model simulates plant performance by modeling each plant component individually, which can take considerable time and effort. The system-based model simulates the plant power with one function. This method involves correlating overall cooling plant power consumption using a quadratic function form. Braun (1989) developed an effectiveness model for cooling towers and cooling coils whose results are in agreement with those of a more detailed numerical solutions study. Braun's model was simple and accurate for design and system simulations. (Braun 1989)

Following Braun's study, Ahn and Mitchell (2001) modelled the central plant components to optimize controls so that the energy consumption is minimized while maintaining comfort conditions in the buildings. The controlled variables are the set temperatures for supply air, chilled water and condenser water, while the uncontrolled variables are load, wet bulb temperature and sensible heat ratio. Using quadratic least square regression techniques, the total cooling plant power is predicted as a function of

the controlled variables mentioned above. The model shows a good fit to data collected under a variety of controlled and uncontrolled variables. (Ahn 2001)

In the year 2000, Gordon and Ng introduced a simple regression model to simulate chiller performance of both mechanical and absorption chillers. The first model introduced includes in its calculations refrigerant measurements. There is not a non-intrusive way to obtain these measures; thus, the model is then presented in terms of coolant measurements. The chiller model is in terms of chilled water leaving temperature, condenser water entering temperature and water flow, and the heat transfer in the evaporator. The predicted values obtained through the regression model presented by Gordon and Ng (2000) showed a good fit to the experimentally measured values. (Gordon 2000)

Following this, Zhang and Turner (2012) made a forward simulating model for a chiller plant without storage, in order to estimate the savings of each measure taken to improve the plant efficiency. The model was based on a water-to-wire plant efficiency concept and is equipment performance-oriented. The Gordon-Ng model is used to simulate chiller performance. Pumps head and efficiency can be simulated as a function of pump flow rate or be constant. A simple cooling fan power model is proposed to calculate the cooling tower wire to water performance. A linear model regressed from trended data was used to simulate the loop delta-T. However, air side parameters are not included in the analysis due to diversity and unpredictability. Zhang and Turner (2012) applied their model to the DFW Airport's Central Utility Plant. The variables optimized where the following: chilled water (ChW) leaving temperature, condenser approach

temperature, and condenser water (CW) flow rate, yielding savings of 3.3% compared to the baseline. (Zhang 2010)

Refrigeration cycles and types of chillers

Refrigeration cycles explain the thermodynamic process that occurs in chillers. Thus, it is important to study these cycles to better understand chiller behavior. There are two types of chillers: mechanical and absorption chillers. Even though they work differently they apply the same refrigeration cycle principles.

Reversible Carnot refrigeration cycle

The Carnot cycle is a reversible thermodynamic cycle formed by two isothermal processes and two isentropic processes. The four branches portrayed in figure 1 represent the processes in the cycle. Process 1-2 is the work input adiabatically compressing the refrigerant and increasing its temperature; in process 2-3, the refrigerant rejects heat isothermally to a hot reservoir; process 3-4 is where the refrigerant expands adiabatically; and finally, in process 4-1 the refrigerant removes heat from the cold reservoir at a constant temperature. Then, the process repeats cyclically.

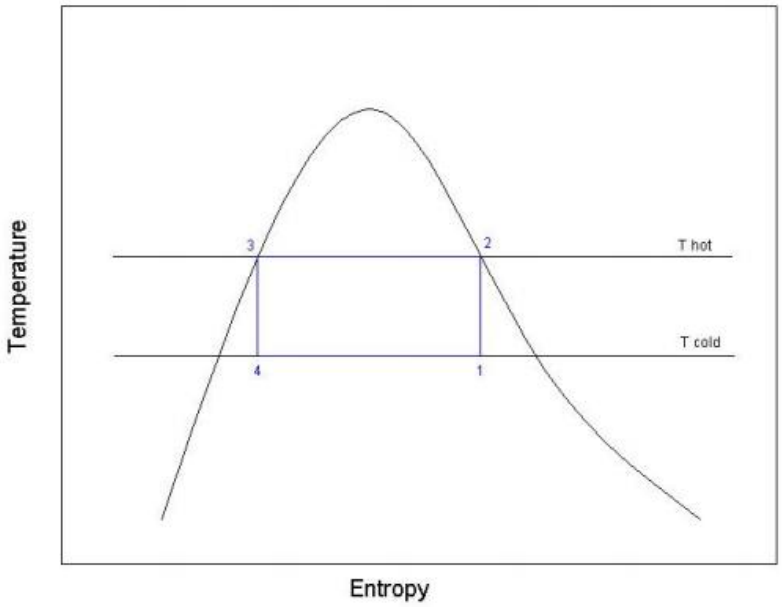

Figure 1. T-s diagram for the Carnot cycle. (Graves 2003)

The Carnot refrigeration cycle represents the maximum possible cooling energy delivered per unit of work because the compression and expansion processes are isentropic; all the heat transfer occurs isothermally and no irreversibilities are introduced.

Thus, the Carnot cycle is ideal and therefore limiting in its representation of a real cooling process. For this reason, the Carnot refrigeration cycle coefficient of performance (COP), which is the cooling capacity divided by the input power as shown in equation 1, will denote the upper bound for a real cycle COP. (Gordon 2000)

$$COP = \frac{cooling\ capacity}{work\ \ input} = \frac{Q_{cold}}{W}$$

Equation 1

$$COP_{Carnot} = \frac{T_{cold}}{T_{hot} - T_{cold}}$$

Equation 2

Vapor compression ideal cycle

Since the Carnot cycle has the highest possible COP, it is expected to try to mimic this cycle as much as possible, taking into account the physical limitations. The vapor compression cycle is a real cycle that overcomes the physical limitations of the Carnot's cycle. The main limitation of the Carnot's cycle is that expansion devices have difficulty handling two-phase mixtures. This limitation cannot be avoided because in order to maintain the isothermal conditions for heat absorption and rejection, the expansion processes cannot be performed outside the dome (saturation region).

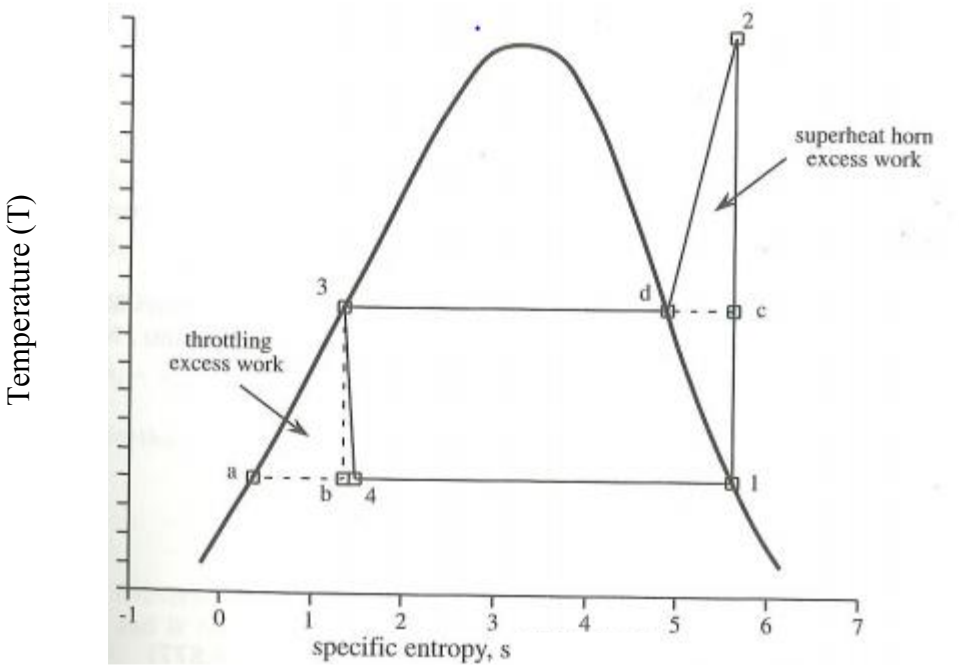

Figure 2. T-s diagram for ideal vapor compression cycle. (Gordon 2000)

The four processes illustrated in figure 2 are the following: 1-2 process is the refrigerant's dry compression and superheating; in process 2-3 the refrigerant rejects heat isobarically; process 3-4 is where the refrigerant expands by isenthalpic throttling, still adiabatic although not isentropic, which represents an introduced irreversibility; and in process 4-1 the refrigerant removes heat isothermally. (Boles 2006)

Vapor compression real cycle

A schematic of a real refrigeration cycle is shown in figure 3 and the temperature - entropy (T-s) diagram is represented is figure 4. The process 1-2, represented in the T-s

diagram, shows the refrigerant compression and discharge to the condenser. Due to precision required in controlling, the refrigerant state is difficult to ensure. Since the refrigerant must be one phase before entering the compression device, and there is no precise way to ensure that the refrigerant enters the device as dry saturated vapor, the refrigerant is usually superheated. Process 2-3 shows the refrigerant de-super heating and condensation by heat rejection. Ideally, the refrigerant should leave the condenser as a single phase saturated liquid but this may not be possible due to pressure losses. Process 3-1 shows the expansion of the refrigerant in a throttling device. Process 4-1 shows the evaporation of the refrigerant by heat removal of the refrigerated space. (Gordon 2000)

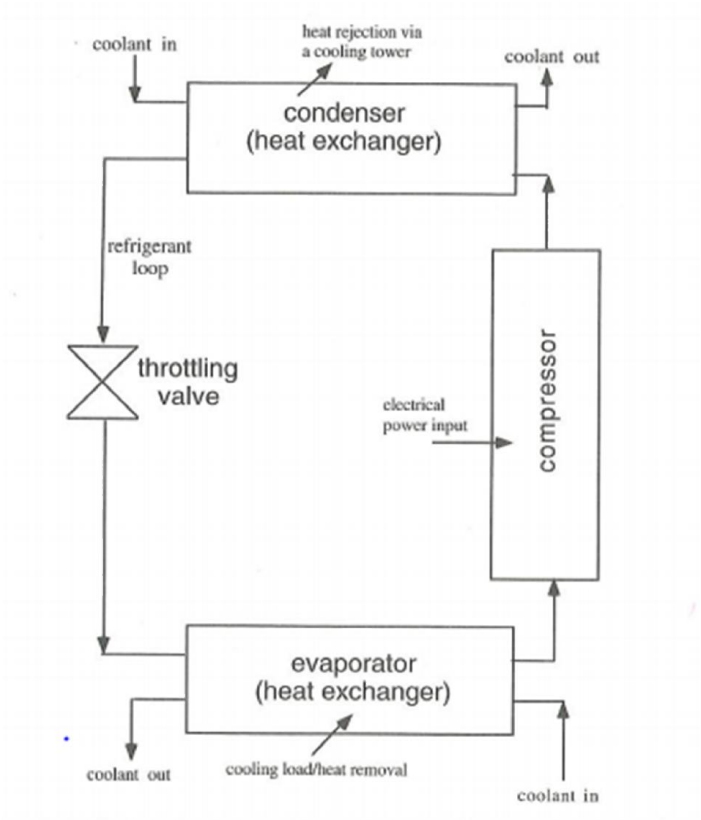

Figure 3. Schematics for real refrigeration cycle. (Gordon 2000)

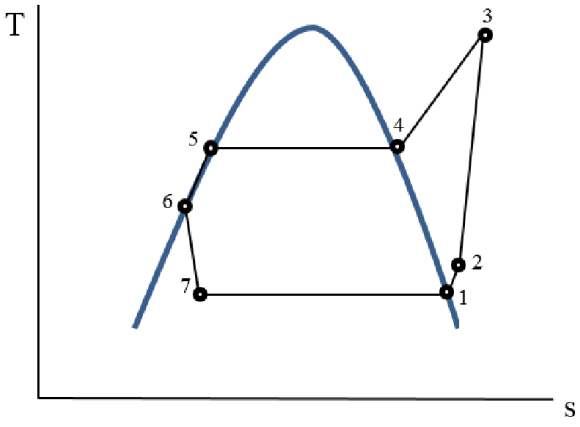

Figure 4. T-s diagram for a real refrigeration cycle

Chiller types

There are two main types of chillers: mechanical and absorption chillers. The schematic shown in figure 3 is common to all mechanical chillers. Moreover, there are various mechanical chillers that vary based on the type of compressor used; some of these are: reciprocating, centrifugal and screw compressor chillers.

Although absorption chillers are similar to mechanical chillers in using a condenser, evaporator and expansion device, they do not use a work-driven compressor. Instead, absorption chillers use thermal power to convert the low-pressure vapor that exits the evaporator into the high-pressure vapor that enters the condenser. The absorption system also includes two additional heat reservoirs: a generator and an absorber.

Absorption chillers work with a refrigerant and a carrier solution that mixes with the refrigerant during part of the process. The refrigerant and the carrier solution are partially separated by the heat input in the generator and then recombined in an exothermic process in the absorber. The absorber and the condenser, work as heat rejection units. Figure 5 shows a schematic for an absorption chiller.

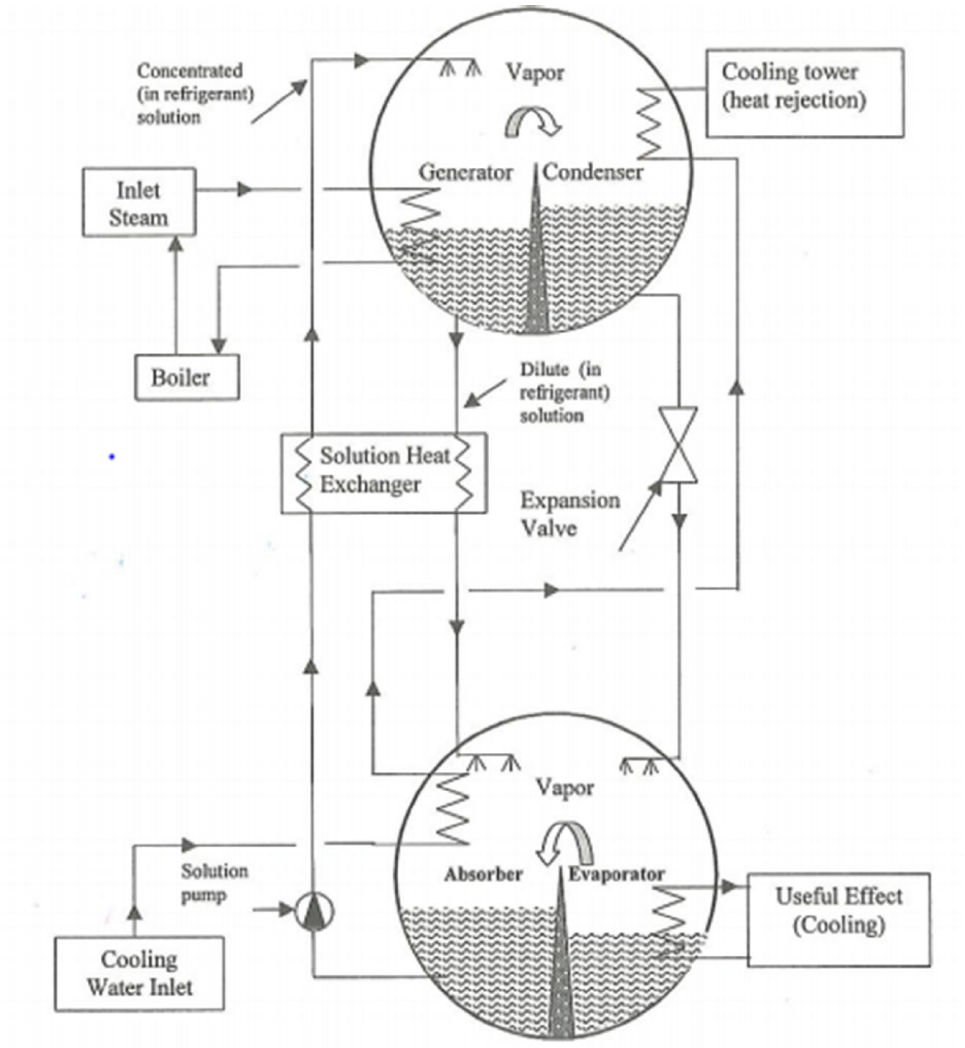

Figure 5. Schematic for an absorption chiller cycle. (Gordon 2000)

The COP for absorption chillers is defined as following

$$COP_{chiller} = \frac{cooling\ rate}{thermal\ power\ input} = \frac{heat\ transfer\ at\ the\ evaporator}{heat\ input\ at\ the\ generator}$$

Equation 3

All chillers have irreversibilities or losses; these irreversibilities are defined thermodynamically by entropy. These losses are classified into 3 general classes: external, internal and heat leaks. External losses derive from the finite rate of heat transfer between the refrigerants and the coolants. Internal refers to the entropy production that does not stem from the chiller interaction with its environments. Finally, heat leaks are the heat transfer between the refrigerant and its surroundings. (Gordon 2000)

In conclusion, a significant part of the energy consumed in the commercial sector is for cooling purposes and chillers are the largest energy consumers in chilled water plants. The commercial sector energy consumption in the US is over 1,300 trillion Btu a month, according to the US Energy Information Administration (2014). Thus, they have been the objective of study for optimization to achieve energy savings. ((EIA) 2014)

CHAPTER III

METHODOLOGY

This study aims to investigate the causes of the low delta-T syndrome in the DFW Airport through the development of a computational model to simulate the chillers and cooling towers of the plant. The plant components were modeled separately and integrated based on their plant operability. The model was fitted to real plant data and simulated the real system. The system simulation was used to find optimal operation conditions. The model input values that would improve the system delta-T and the plant's overall performance were found via an iterative process.

In addition, plant data was analyzed to investigate the current plant control operations. Current data analysis results served as a starting point to evaluate different variables that can cause the low delta-T problem.

The system simulation was comprised of a chiller model, cooling tower model, pump model, loop delta-T model and a tank model. Finally, the optimization strategy was developed to minimize the power consumed by the chillers, cooling tower fans and condenser pumps while increasing plant delta-T and meeting the cooling requirements. The plant optimization was accomplished with an iterative process that determined the values of the input variables, so that energy savings were maximized for different operating conditions. New setpoints for the optimized variables were recommended, in order to improve the plant's performance.

Chiller modeling

Chilled water plants account for a large part of building energy consumption and chillers consume the majority of plant power. Moreover, chiller performance directly impacts chiller operation. For these reasons, is important to ensure efficient chiller operation.

Chiller performance can vary depending on different parameters such as chilled water leaving temperature, condenser water flow rate and entering temperature, and partial load conditions. Thus, chiller performance is complex and vital to ensure good performance of the system as a whole. The model proposed by Gordon et al (2000) is used to simulate chiller performance. This thermodynamic model is expressed in terms of readily measured coolant temperatures, as opposed to refrigerant temperatures.

The starting points to derive this thermodynamic chiller model are the first and second law of thermodynamics. It is important to remember that energy and entropy do not change in a cyclic process, thus, following the notation of Gordon et al (2000), we have

$$\Delta E = 0 = Q_{cond} + Q_{cond}^{leak} - Q_{evap} - Q_{evap}^{leak} - P_{in} + Q_{comp}^{leak}$$

Equation 4

$$\Delta S = 0 = \frac{Q_{cond} + Q_{cond}^{leak}}{T_{cond}} - \frac{Q_{evap} + Q_{evap}^{leak}}{T_{evap}} - \Delta S_{int}$$

Equation 5

Where:

ΔE change of internal energy over one cycle

ΔS change of entropy over one cycle

Q_{cond} heat exchanged in the condenser

Q_{cond}^{leak} heat leak at the condenser

Q_{evap} heat exchanged in the evaporator

Q_{evap}^{leak} heat leak at the evaporator

P_{in} input power

Q_{comp}^{leak} heat leak at the compressor

ΔS_{int} rate of internal entropy production

Combining the first and second laws of thermodynamics with the coefficient of performance (COP), we have

$$COP = \frac{Q_{evap}}{P_{in}}$$

Equation 6

$$\frac{1}{COP} = -1 + \frac{T_{cond}}{T_{evap}} + \frac{T_{cond}\Delta S_{int}}{Q_{evap}} + \frac{T_{cond}}{Q_{evap}}\left[Q_{evap}^{leak}\left(\frac{1}{T_{evap}} + \frac{1}{T_{cond}}\right) + \frac{Q_{evap}^{leak}}{T_{cond}}\right]$$

Equation 7

However, these are refrigerant temperatures, which cannot be measured non - intrusively. To use coolant measures, instead of refrigerant measures, heat exchanger energy balance equations are used

$$Q_{cond} = (mCE)_{cond}\left(T_{cond} - T_{cond}^{in}\right) = \frac{(mCE)_{cond}}{1 - E_{cond}}\left(T_{cond} - T_{cond}^{out}\right)$$

Equation 8

$$Q_{evap} = (mCE)_{evap}\left(T_{evap}^{in} - T_{evap}\right) = \frac{(mCE)_{evap}}{1 - E_{evap}}\left(T_{evap}^{out} - T_{evap}\right)$$

Equation 9

Equations 7, 8 and 9 are combined and simplified to obtain

$$\frac{T_{evap}^{in}}{T_{cond}^{in}}\left(\frac{1}{COP} + 1\right) = 1 + \frac{T_{evap}^{in}\Delta \boldsymbol{S_{int}}}{Q_{evap}} + \frac{\boldsymbol{Q_{eqv}^{leak}}\left(T_{cond}^{in} - T_{evap}^{in}\right)}{T_{cond}^{in} Q_{evap}} + \frac{\boldsymbol{R}\, Q_{evap}}{T_{cond}^{in}}\left(\frac{1}{COP} + 1\right)$$

Equation 10

Where

$$R = \frac{1}{(mCE)_{cond}} + \frac{1}{(mCE)_{evap}}$$

Equation 11

$$Q_{eqv}^{leak} = Q_{evap}^{leak} + \frac{Q_{comp}^{leak} T_{evap}^{in}}{T_{cond}^{in} - T_{evap}^{in}}$$

Equation 12

$\Delta S_{int} Q_{eqv}^{leak}$ and R represent irreversibilities in the form of internal dissipation, heat leaks and finite rate heat exchange, respectively. These three parameters are found through multiple-linear regression to equation 10.

This model however, doesn't include coolant flow rates. Most older commercial chillers were designed to operate at constant coolant flow rates. Nevertheless compressor power consumption can change when chillers operate at variable coolant flow rate. For this reason, coolant flow (specifically coolant flow in the condenser) is incorporated as an additional control variable.

In the interest of adapting the model in equation 10 to include coolant flow rate, the overall thermal resistance R can be expressed in terms of coolant flow rate, specific heat density and heat exchanger effectiveness for the evaporator and condenser.

$$R = R_{cond} + R_{evap} = \frac{1}{(V\rho CE)_{cond}} + \frac{1}{(V\rho CE)_{evap}}$$

Equation 13

Since chiller output temperature is usually reported in terms of chilled water leaving temperature T_{evap}^{out}, the evaporator effectiveness is changed to the following:

$$R = \frac{1}{(V\rho CE)_{cond}} + \frac{1 - E_{evap}}{(V\rho CE)_{evap}}$$

Equation 14

Combining and simplifying equations 10 and 14, we obtain

$$\frac{T_{evap}^{out}}{T_{cond}^{in}}\left(\frac{1}{COP} + 1\right) = 1 + \frac{T_{evap}^{out}\Delta \boldsymbol{S_{int}}}{Q_{evap}} + \frac{\boldsymbol{Q_{eqv}^{leak}}\left(T_{cond}^{in} - T_{evap}^{out}\right)}{T_{cond}^{in}Q_{evap}} + \frac{Q_{evap}}{T_{cond}^{in}}\left(\frac{1}{COP} + 1\right)\left(\frac{1}{(V\rho C)_{cond}} + \boldsymbol{R'}\right)$$

Equation 15

Where:

$$R' = \frac{1 - E_{evap}}{(V\rho CE)_{evap}}$$

Equation 16

These three parameters in equation 15, $\Delta S_{int} Q_{eqv}^{leak}$ and R' **,** can be obtained similarly through multiple-linear regression.

Using the three parameters found using the multiple linear regression, the chiller power can be predicted using the following equation:

$$P_{in} = \left[\frac{1 + \frac{T_{evap}^{out} \Delta \boldsymbol{S_{int}}}{Q_{evap}} + \frac{\left(T_{cond}^{in} - T_{evap}^{out}\right)}{T_{cond}^{in} Q_{evap}} \boldsymbol{Q_{eqv}^{leak}}}{\frac{T_{evap}^{out}}{T_{cond}^{in}} - \frac{Q_{evap}}{T_{cond}^{in}} \left(\frac{1}{(V \rho C)_{cond}} + \boldsymbol{R} \right)} \right] Q_{evap}$$

Equation 17

Figure 6 shows a diagram where all the variables mentioned above are located and measured. (Gordon 2000)

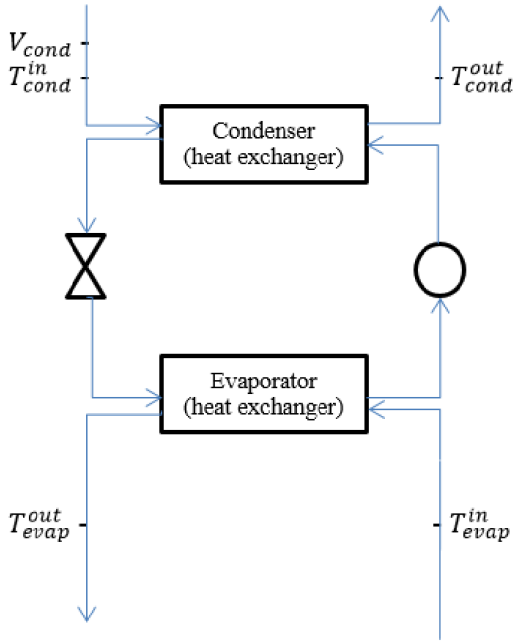

Figure 6. Schematics for the chiller components and variable location

Where:

V_{cond} water flow going through the condenser

T_{cond}^{in} water temperature entering the condenser

T_{cond}^{out} water temperature leaving the condenser

$\boldsymbol{T_{evap}^{out}}$ water temperature leaving the evaporator

$\boldsymbol{T_{evap}^{in}}$ water temperature entering the evaporator

Pump modeling

The Energy Systems Laboratory (ESL) has previously performed a study on DFW Airport's central plant. Part of the study evaluated the operational costs of secondary pumps and secondary pumps combined with tertiary pumps. To evaluate the operational costs, the ESL developed a mathematical model that describes the relationship between pumping power and chilled water flow. This model was based on 2010 measured energy consumption data peak and partial water flow conditions. Results are as follows:

$$\text{Pump power (kW)} = 0.00000128(\text{ChW flow})^2 + 0.0007(\text{ChW flow}) + 24.024$$

Equation 18

Where:

ChW chilled water

The water flow rate is measured in gallons per minute (gpm) to obtain the pumping power in kilowatts (kW).

DFW Airport will be undergoing an expansion, adding stingers to terminals A and D, a terminal B-D connector, a terminal E satellite and the Business Tower addition. Potential load increases for terminals A, B, C and E were also calculated, based on data provided by DFW Airport for the design load for terminal A. The other terminals were assumed to increase by the same ratio.

A new mathematical model was developed for the calculated increased loads, yielding the following equation:

$$\text{Pump power (kW)} = 0.0000018(\text{ChW flow})^2 - 0.004(\text{ChW flow}) + 49.37$$

Equation 19

The data set used in the DFW Airport CUP study done by the ESL in 2010 is compared to the data sets from 2012-2013, which is the one being used in this thesis. It was determined that the plant is still working under the same conditions as it was in 2010. That is, the DFW Airport has not completed the proposed expansions. Therefore, the relationship used to predict pump power consumption is the one presented in equation 18. ((ESL) 2011)

Cooling tower simulation

Thermal performance of a cooling tower largely depends on the entering air wet bulb temperature. The entering air dry-bulb temperature and relative humidity have an insignificant effect on thermal performance of mechanical draft cooling towers, but affect the rate of evaporation in the cooling tower.

The approach to the wet bulb, or the approach temperature difference, is the difference between the leaving water and entering air wet bulb temperatures. The approach is a function of cooling tower thermal capability. Usually, the larger the cooling tower, the closer the approach temperature is.

The thermal capability of any tower is defined by the following parameters: entering and leaving water temperatures, entering air wet bulb and dry bulb temperatures and water flow rate. The cooling tower performance curves describe how the combinations of flow rate and heat load determine the cooling tower range; that is, the temperature difference between the water entering and leaving the cooling tower. The entering air wet bulb and desired leaving water temperatures combine with cooling tower size to balance the heat rejected at a specific approach. Performance curves describe the relationship between the water leaving temperature, the wet bulb temperature and temperature range for a given tower.

The theory proposed by Baker and Shyrock (1961) is the most common model for cooling towers and involves a great number of iterations. Thus, an alternative way is used to describe the cooling tower behavior. The approach temperature was set based on

the DFW Airport's existing cooling tower design parameters and existing leaving water temperature setpoints.

Secondary loop water delta-T simulation

To study the low delta-T syndrome, a model was built to simulate the delta-T behavior under different conditions. The loop delta-T was simulated with a regression model based on the water side parameters and temperature data. Air side variables are not considered in the model because they are numerous and unpredictable. In the DFW Airport there are hundreds of Air Handling Units (AHUs) working with different configurations and coils in different conditions. Consequently, including air-side parameters in a model is a difficult and time consuming task; thus, the loop delta-T simulation model is currently restricted to the water-side parameters, air dry bulb and wet bulb temperatures.

A regression model for DFW Airport secondary loop delta-T was first developed by Zhiquin Zhang in 2010. In this study, the more appropriate variables for the regression were determined using the Statistical Analysis System (SAS) software. The objective was to consider the variables that maximized R^2_{adj} also taking into account Cp which is the total mean square error for the regression model. Thus, a viable regression variable would be one that maximizes R^2_{adj} and has a minimum Cp or a slightly larger Cp which do not contain much bias. The best regression equation to model the loop delta-T yielded in that study was:

$$\Delta T = a_3 ChWST + a_2 Twb + a_1(cooling\ load) + a_0$$

Equation 20

The system linear model used in this thesis was regressed from DFW Airport data. (Zhang 2010)

Thermal Energy Storage tank behavior simulation

The Thermal Energy Storage (TES) tank is an important part of the DFW Airport cooling system, especially in the summer months. During the months of June, July, August and September the TES tank fully provides chilled water for the DFW Airport from 3 pm to 6 pm due to rate structures. The DFW Airport staff provided a detailed monthly bill of the DFW Airport chilled water plant shown in Appendix B. However, the complete rate schedule is not available. Based on this bill, it appears that there would be an additional charge of at least $3.33/kWh, for each kW of energy consumed by a chiller that came on during the 3 pm to 6 pm period. For this reason it is very important to ensure that the tank capacity will be large enough to provide the additional water needed to meet the cooling loads, especially in the summer months.

A tank model was built to predict the ratio of chilled water in the tank to guarantee enough chilled water to meet the airport's cooling loads. Zhang (2010) proposed a relationship for the chilled water ratio in the tank that uses the amount of chilled water present in the tank and the amount of chilled water being charged or discharged from the tank to calculate the existing amount of chilled water in the tank.

The following equation was used in this study to predict the chilled water level in the tank:

$$x_{ChWtank} = \frac{V_{ChW}}{V_{total}}$$

Equation 21

$$x_{ChWtank} = {x_{ChWtank}}^{-1} + \frac{\dot{V}_{ChW} * t}{V_{total}}$$

Equation 22

Where:

$x_{ChWtank}$	chilled water ratio in the tank
V_{ChW}	tank chilled water volume
V_{total}	tank total volume capacity
${x_{ChWtank}}^{-1}$	tank chilled water ratio from the previous time stamp
$\dot{V}_{ChW}$	volumetric flow rate of chilled water in and out of the tank
t	time period over which the tank volumetric flow rate is measured

The volumetric flow rate of chilled water is determined by comparing the volumetric flow rate in the primary and secondary loop. The secondary loop water flow will vary depending on the chilled water supply temperature setpoint. (Zhang 2010)

Optimization process

The three different models were built to find the best value for the most significant chilled water plant variables such as chilled water leaving temperature (ChWST), condenser water flow, and approach temperature. Using searching algorithms, the best values were found so that the plant energy consumption was minimized.

In addition, optimized variables were restricted by upper and lower limits due to machinery constraints. These limits were set to ensure good performance, and more importantly that the results found were applicable to the chilled water central plant.

The chiller model developed for the chiller current operation was used to carry out a sensitivity study by changing the model's input parameters. The parameters studied for possible modification in order to minimize chiller consumption were the cooling tower approach temperature, the chilled water leaving temperature and the water flow through the condenser and cooling towers.

The values of these three variables were changed within an optimal working range for the machinery involved. Each one of the variables were changed separately to understand the effect of each variable in the chiller power consumption.

The plant delta-T was simulated using the new chiller working parameters to predict the plant delta-T with the optimized values and calculate the new chilled water requirement for the plant secondary loop.

The secondary pump power simulation was used to predict the pumping power consumption under the new working conditions. The predicted pumping power was compared with the chiller predicted power consumption to obtain net savings.

These new working conditions for the chiller were used to find the TES tank modified cooling capacity and compared to current tank energy consumption. The new chiller variables should still allow the TES tank to provide cooling under the current working operation schedule. This analysis is made with the purpose of finding any other possible limitations for the chillers' optimized working conditions.

CHAPTER IV

RESULTS

System description

The central chilled water system studied for this project is located in the DFW Airport. This is a primary-secondary system consisting of six on-site manufactured (OM) 5,500 ton centrifugal chillers, a 90,000 ton-hr Thermal Energy Storage tank, five 1,350 ton glycol-solution chillers (PCA chillers) and eight two-speed cooling towers. The plant has six 150 hp constant speed primary pumps and four 450 hp variable speed secondary pumps. After running through the secondary pumps, the chilled water is distributed to the terminals and different airport buildings through the main utility tunnel. The supply and return chilled water pipes are 36 inches in diameter. The chilled water (ChW) generated from the CUP is also used to pre-cool the glycol solution prior to entering the PCA chillers. Figure 7 shows a diagram of the chilled water system.

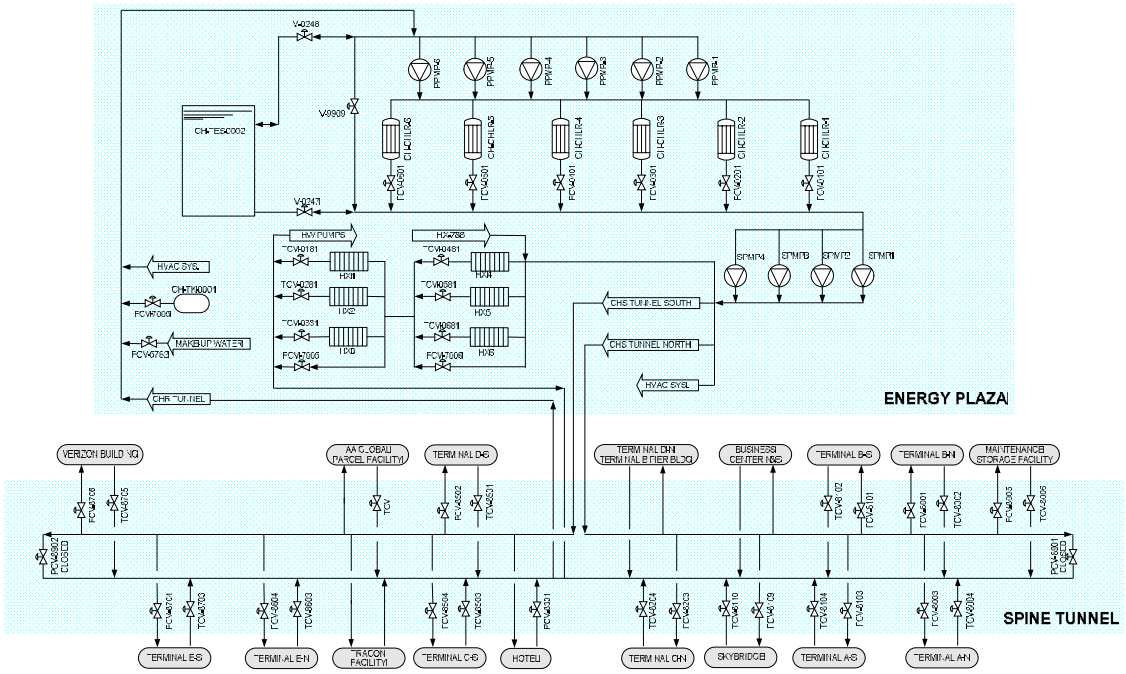

Figure 7. Complete layout of the DFW Airport's Central Plant

The condenser water system consists of 8 cooling towers. Each of these cooling towers has a 150 hp two speed motor fan and a 400 hp condenser water pump. The cooling towers are located to the east and west of the plant, having 4 on each side.

The thermal storage tank is located between the primary pumps' suction side header and the chiller discharge side header. The tank is 138 ft in diameter and 57 ft in height. The tank is also naturally stratified, is open to the atmosphere and the water level is maintained at about 54 ft. The effective storage volume is around 5,400,000 gallons.

Data Analysis

To gain a preliminary understanding of the DFW Airport chilled water system, the plant data was analyzed. The analysis was performed in order to find possible causes for the DFW Airport chilled water low delta-T syndrome and which reset schedules are in place. In the following sections a detailed description of the study is presented.

Plant delta-T

DFW Airport's Central Utility Plant (CUP) experiences low delta-T syndrome, meaning the temperature difference between the supply and return chilled water drops below design value at low loads. The plot in Figure 8 shows how the chilled water delta-T drops significantly when the load gets below 70,000 kBtu/hr. This drop in delta-T roughly coincides with the cool weather period beginning in October and ending in April as shown in Figure 9.

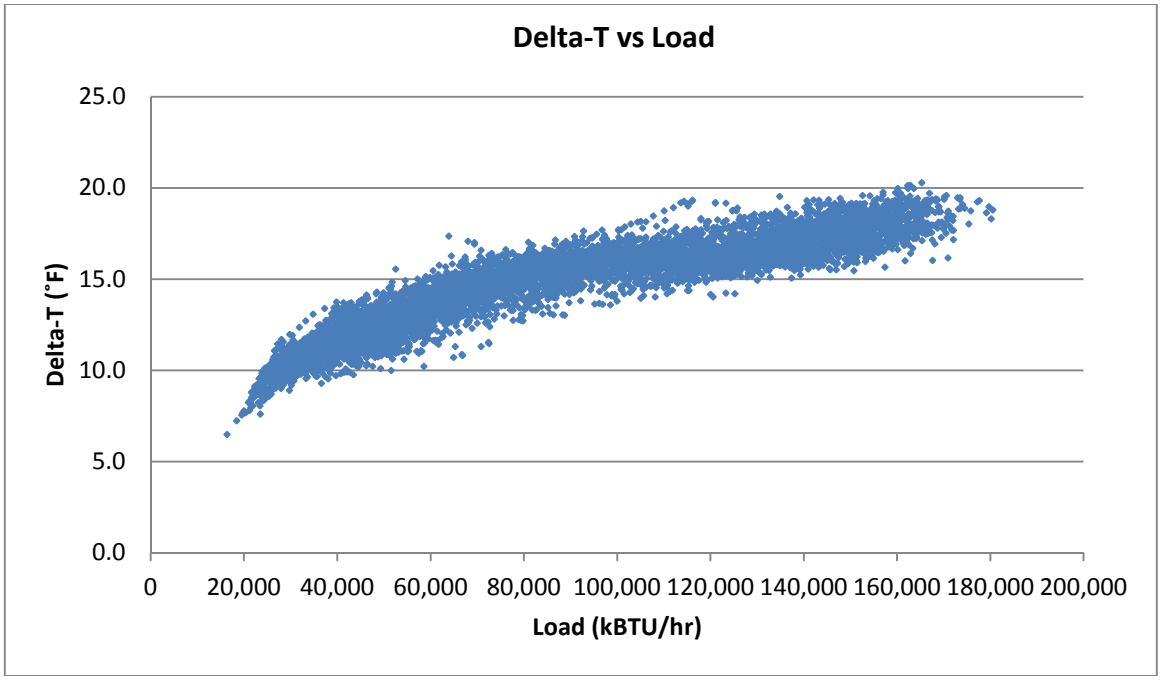

Figure 8. CUP chilled water delta-T vs total cooling loads

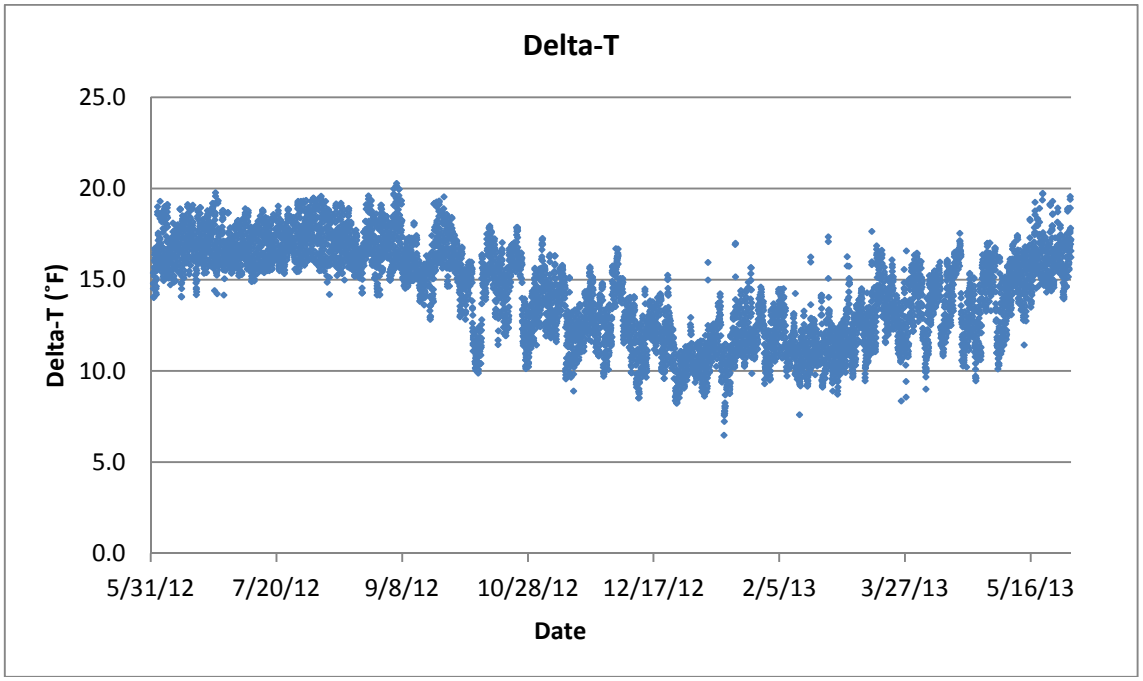

Figure 9. Chilled water delta-T

The cooling load is directly proportional to flow rate and delta-T, as presented in equation 23. Thus, the water flow rate would have to decrease in order to maintain a high delta-T and meet the buildings' cooling loads.

$$\boldsymbol{Q = \dot{m} C_p \Delta T}$$

Equation 23

$$\left(\frac{\boldsymbol{Btu}}{\boldsymbol{h}}\right) = \mathbf{500}\ \boldsymbol{GPM\ \Delta T}$$

Equation 24

Though the chilled water flow rate is directly proportional to the cooling loads, as shown in Figure 10, the delta-T still drops as the cooling loads do. Thus, other reasons such as chilled water supply water temperature, TES tank discharge and cooling tower operation were investigated as possible causes for the low delta-T syndrome.

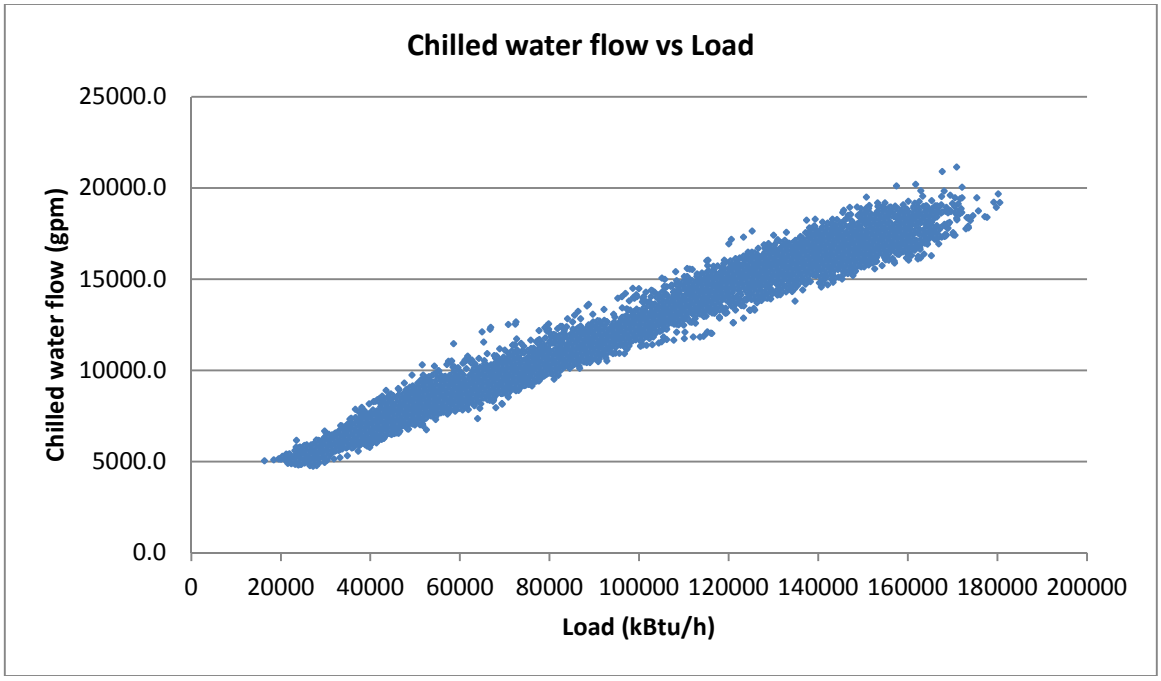

Figure 10. Plant chilled water flow rate vs cooling load

Chilled water supply temperature (ChWST) was analyzed to investigate if it could be a possible reason for the low delta-T syndrome. The noise observed in the plot in figure 11 shows a temperature range between 36˚F and 41˚F for the summer months and from 36˚F to 39˚F for fall and spring months. The range in the winter months was smaller showing a noise of about 1.5˚F.

Since ChWST seems dependent on the outside air temperature (OAT), ChWST was plotted against the OAT. However, as shown in figure 12 there is no dependence between the two.

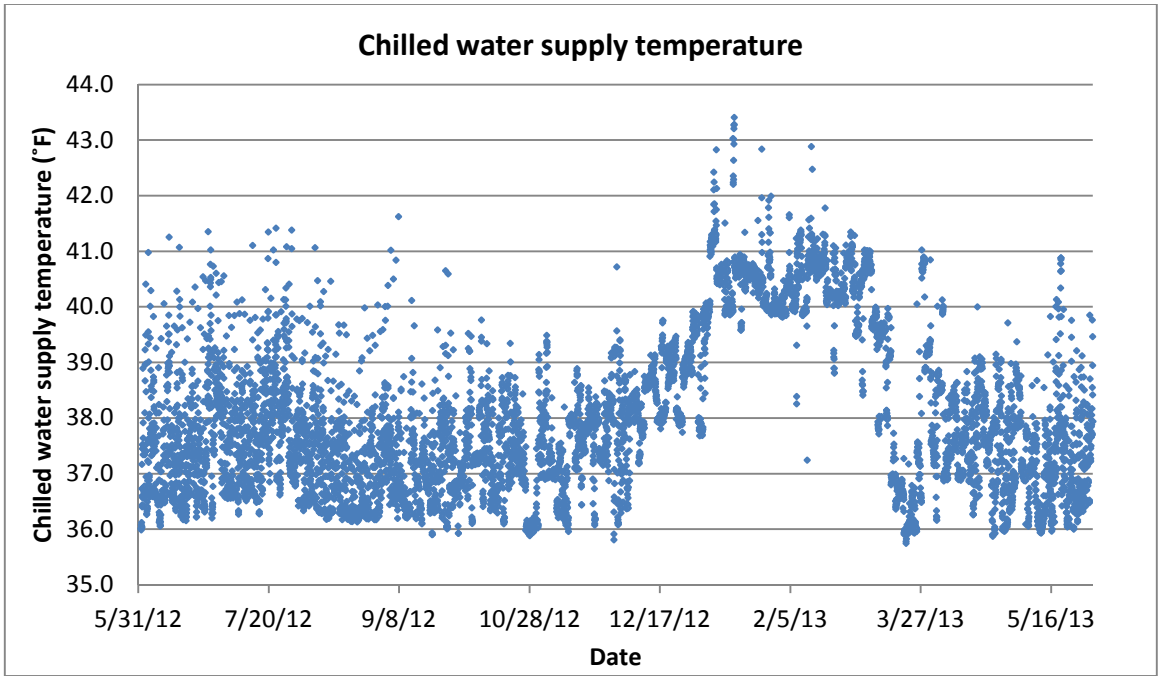

Figure 11. Chilled Water Supply Temperature vs time

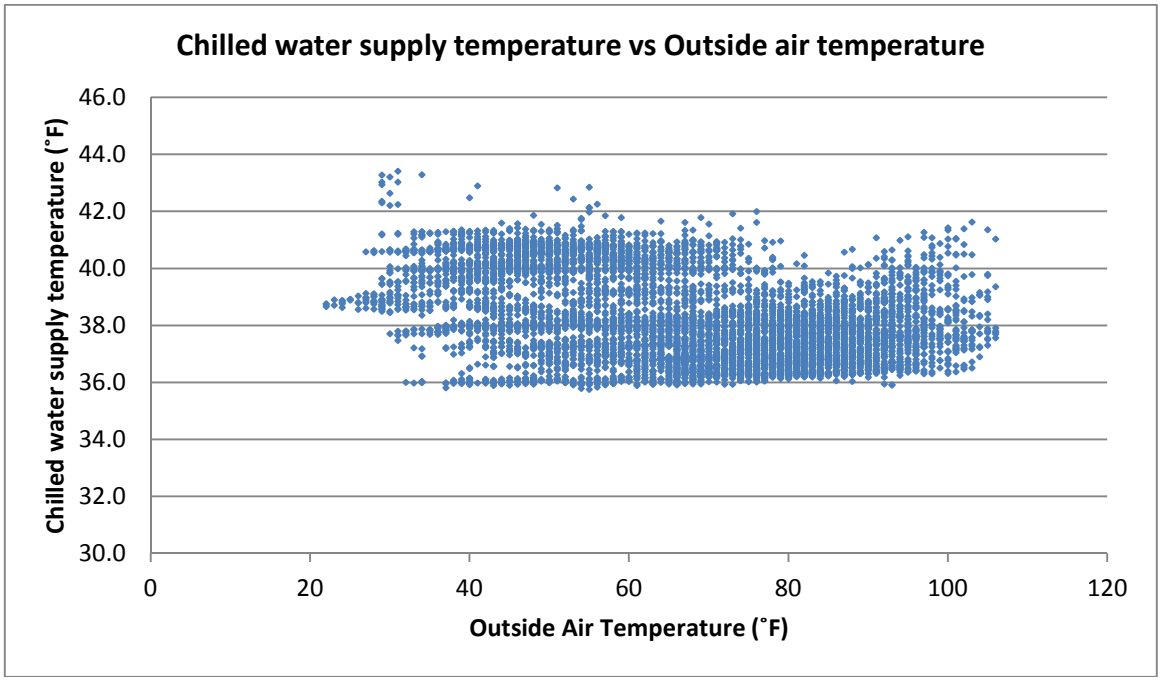

Figure 12. Outside air Temperature dependence of the Chilled Water Supply Temperature

Since the noise in the ChWST is varying with the seasons and there is no dependence on OAT, a detailed monthly study was carried out. The ChWST setpoint changed throughout the year being 36˚F from April to October, 38˚F for November and December and 40˚F from January to March.

These setpoints were inferred by data analysis since the current control sequence for the DFW Airport's CUP was not available for this study. Due to rate structures, all chillers are scheduled to turn off from 15h to 18h (3 pm to 6pm) in the months of June, July, August and September. The TES tank supplies chilled water at the time the chillers are off. For these months the peak ChWST occurs at 6 pm. Figure 13 shows the ChWST during June, and the peak ChWST at 6 pm. Figures 14 and 16 show the ChWST during the months of October to April respectively. These figures illustrate how the peak chilled water temperature occurs at random times, happening at both day and night time. Figure 15 shows the ChWST during January and a ChWST stable behavior. The peak temperature pattern from June 2012 to September 2012 occurs again in May 2013. The noise in the ChWST is correlated with the noise found in the plant delta-T, however, the noise in the ChWST is not a cause for the low delta-T since it occurs in the months were the delta-T is higher.

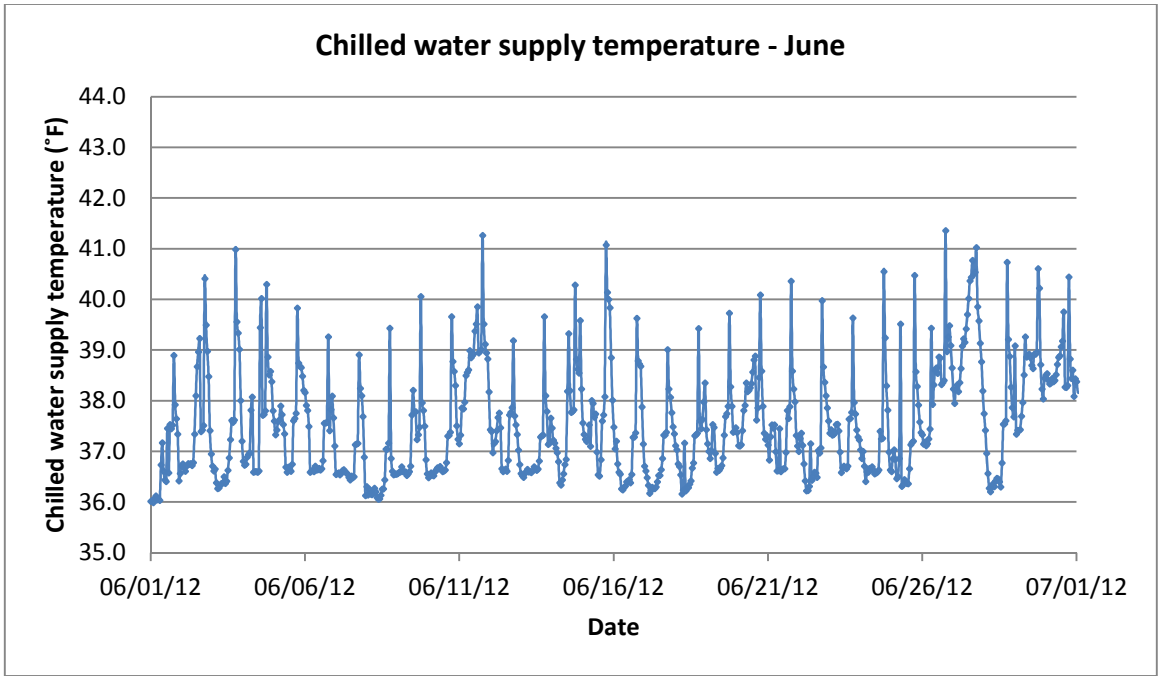

Figure 13. Chilled Water Supply Temperature for June-2012

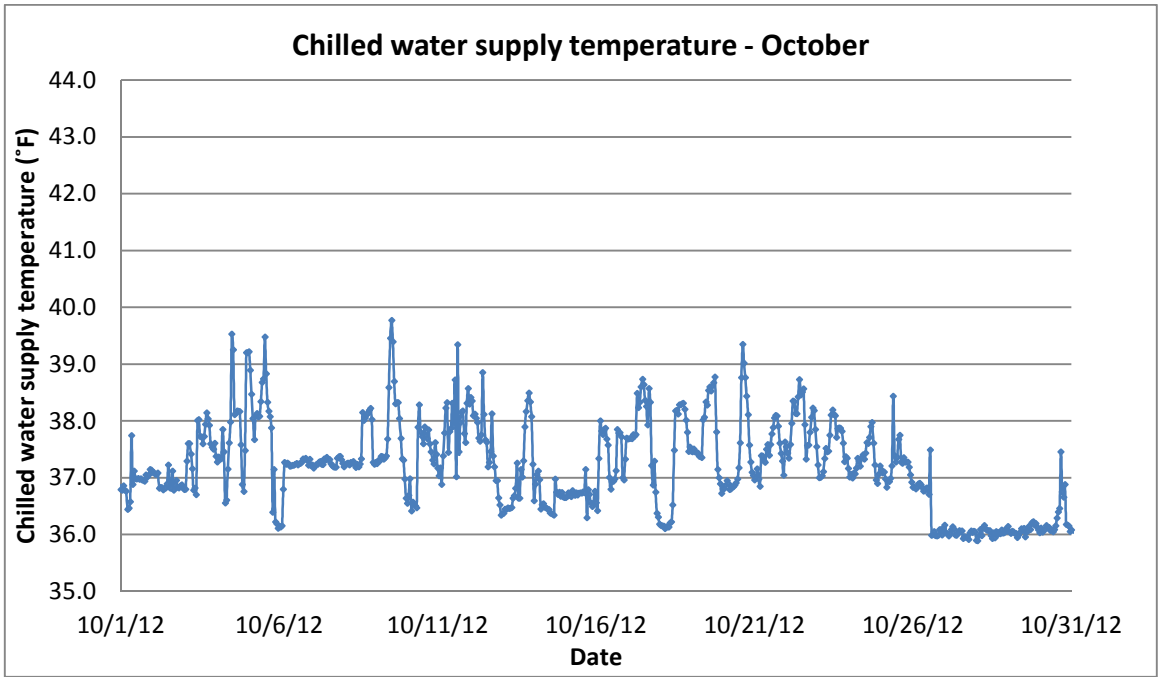

Figure 14. Chilled Water Supply Temperature for October-2012

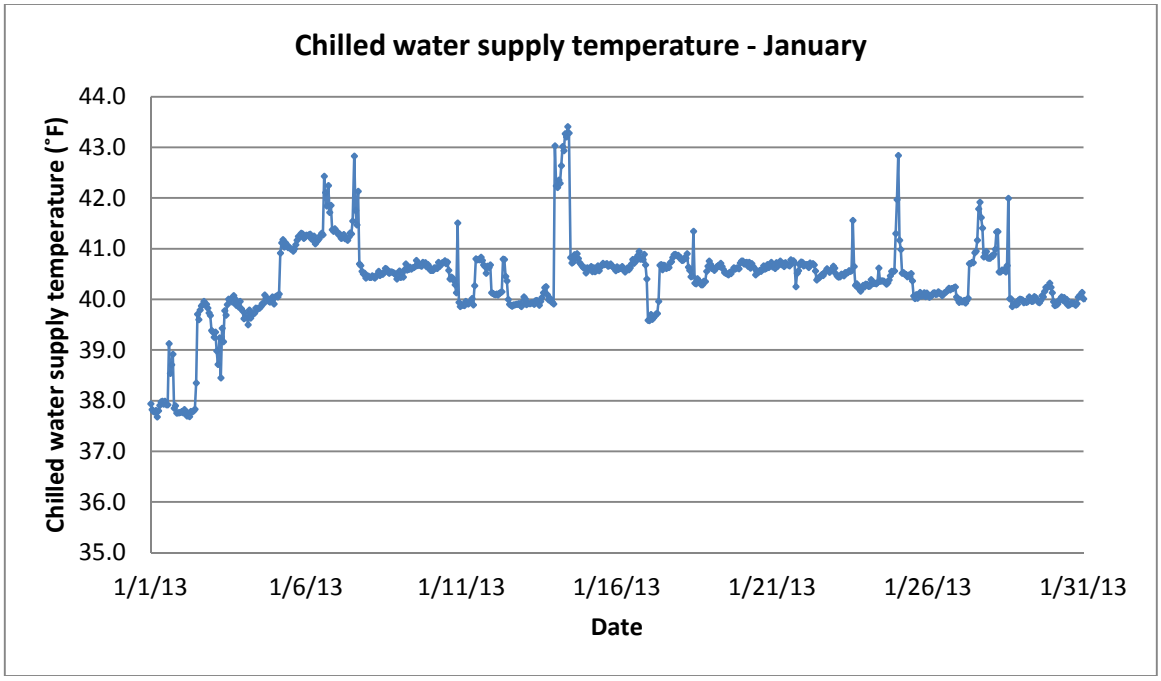

Figure 15. Chilled Water Supply Temperature for January 2013

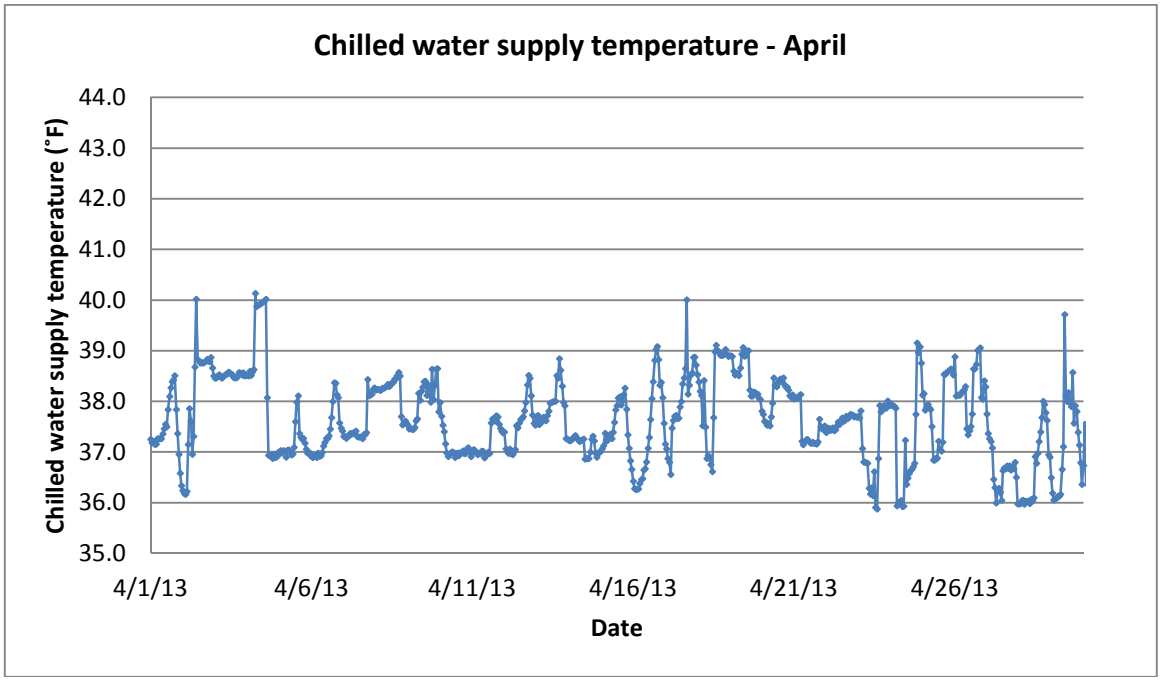

Figure 16. Chilled Water Supply Temperature for April-2013

The TES tank provides chilled water for the airport from 3 pm to 6 pm during the summer months. The TES tank data was analyzed during these months because the peak temperature occurred at 6pm. This analysis was made to find a correlation between the peak of the ChWST and the TES tank discharge temperature. TES tank data was only available since December 2012; thus, the analysis was not made prior to this date (2012 summer months).

The analysis was done choosing one specific day per month. The days were chosen because they had the highest temperature range in the ChWST. Each month, for the day with the highest ChWST peak the TES tank temperature was plotted every two feet for the height of the tank for every hour in the day. Figures 17, 19, 21, 23, 25 and 27, for the months of December through May respectively, show the tank discharge water temperature for every hour of the day. As shown in these figures, water temperature at the TES tank outlet remains constant and close to the ChWST setpoint throughout each day. Thus, the TES tank has no relation to the peak in the ChWST found in the summer months at 6pm. This peak temperature may be due to the chiller schedule. Since the chillers are turned on at 6 pm, it is possible that the chillers are not able to get the chilled water temperature down to the setpoint by the time the measurements are taken.

For the same days, the chilled water flow from the primary loop and the tank discharge were plotted. These plots are shown in figures 18, 20, 22, 24, 26 and 28 for the months of December through May respectively. This was done to visualize how much

chilled water was actually supplied by the TES tank. As observed the TES tank provides more chilled water closer to the summer months.

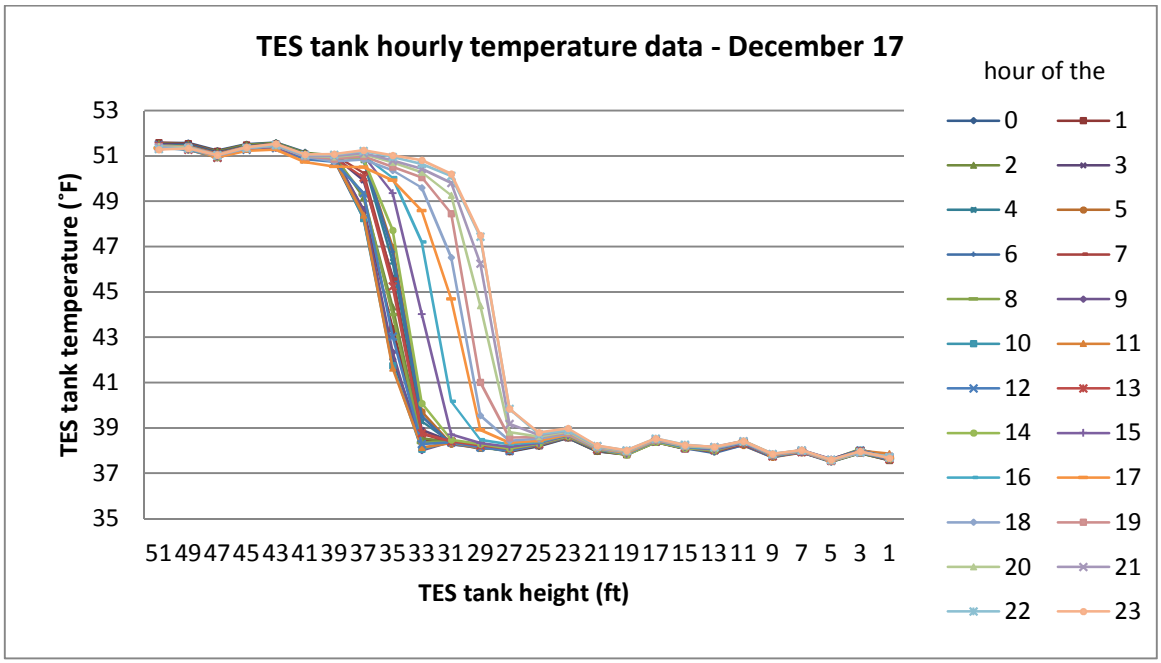

Figure 17. Hourly TES tank temperature data vs tank height for December 17, 2012

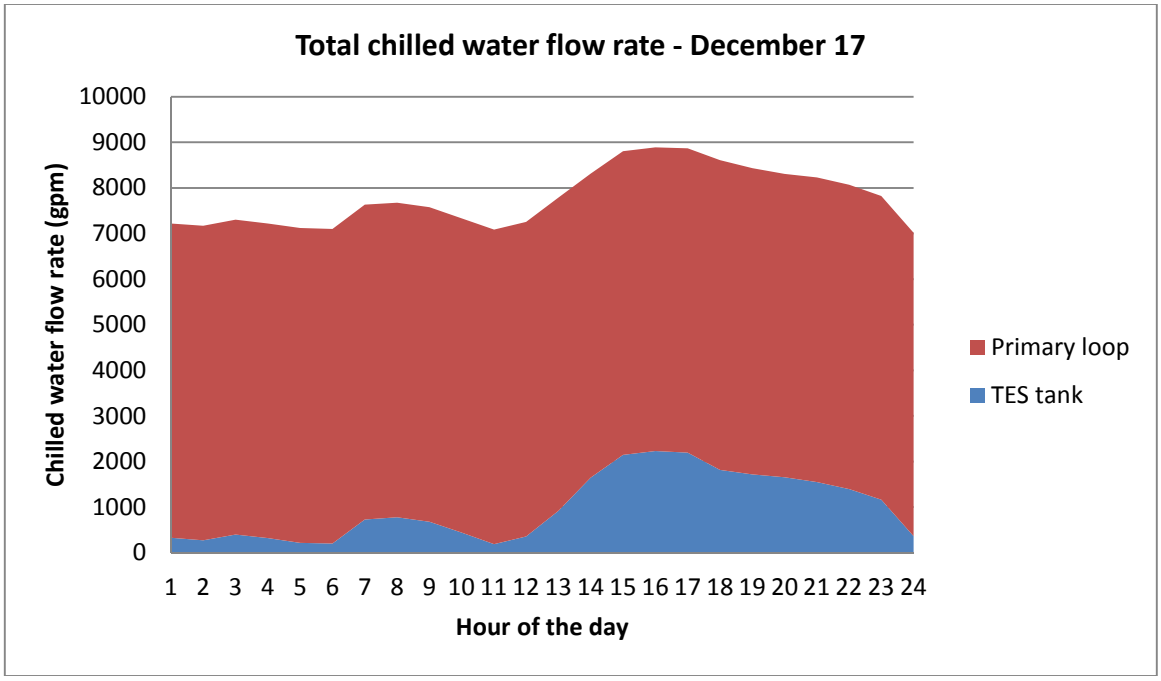

Figure 18. TES tank flow rate compared to the primary loop flow rate for December 17, 2012

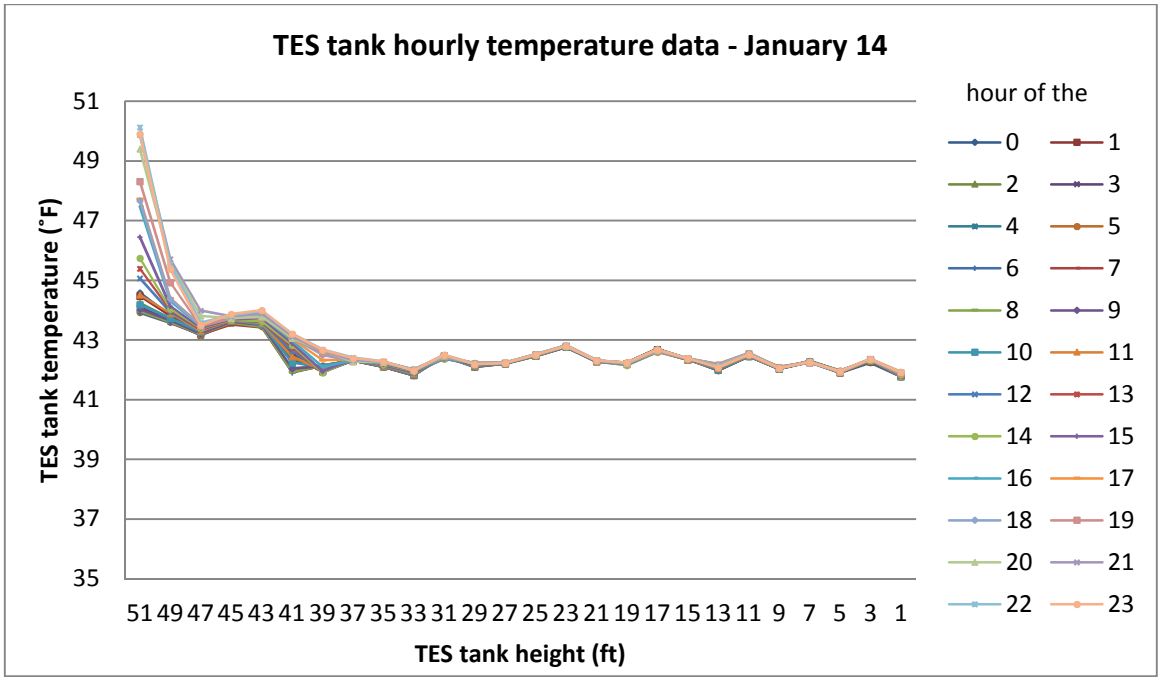

Figure 19. Hourly TES tank temperature data vs tank height for January 14, 2013

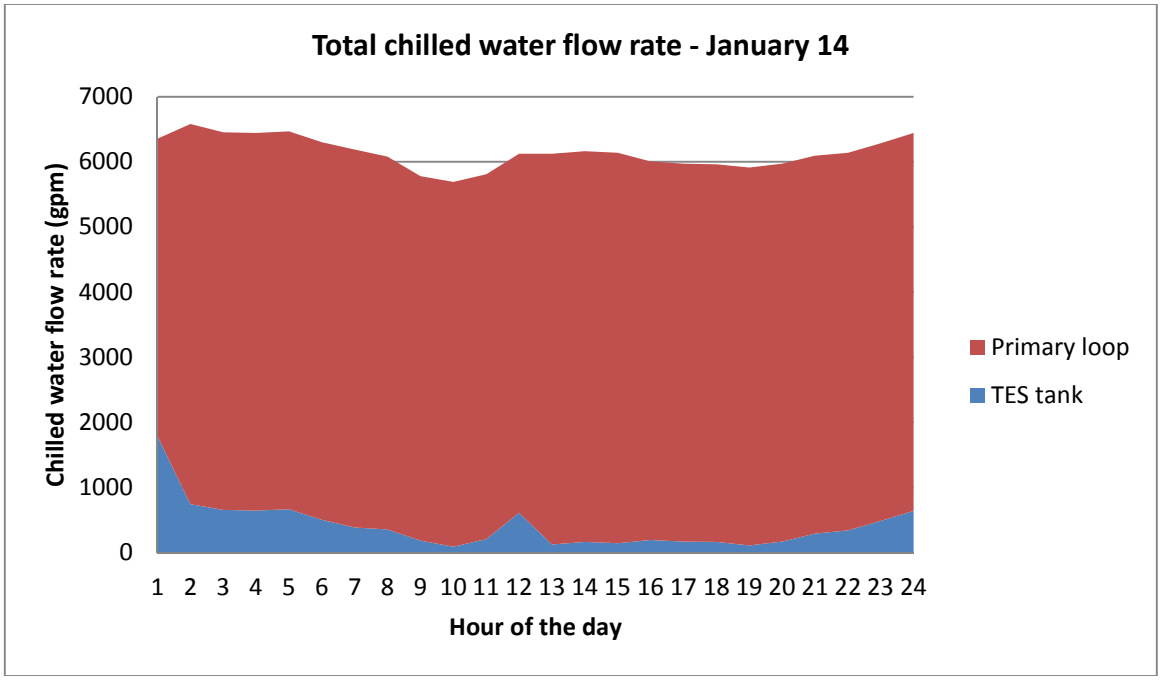

Figure 20. TES tank flow rate compared to the primary loop flow rate for January 14, 2013

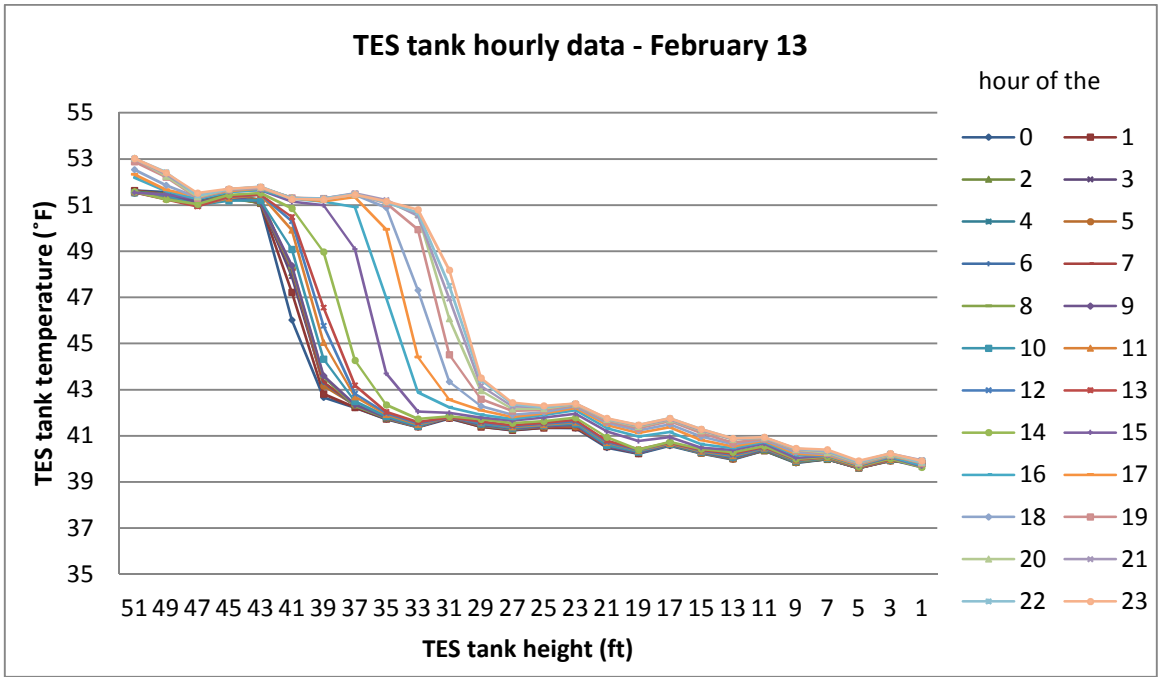

Figure 21. Hourly TES tank temperature data vs tank height for February 13, 2013

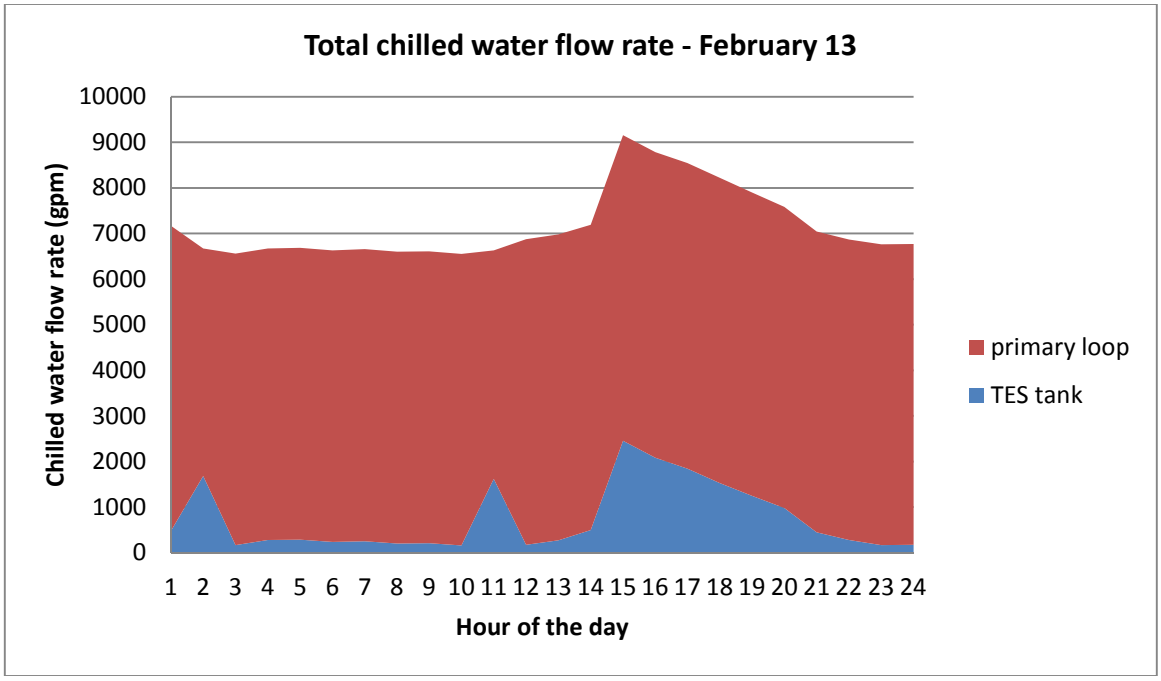

Figure 22. TES tank flow rate compared to the primary loop flow rate for February 13, 2013

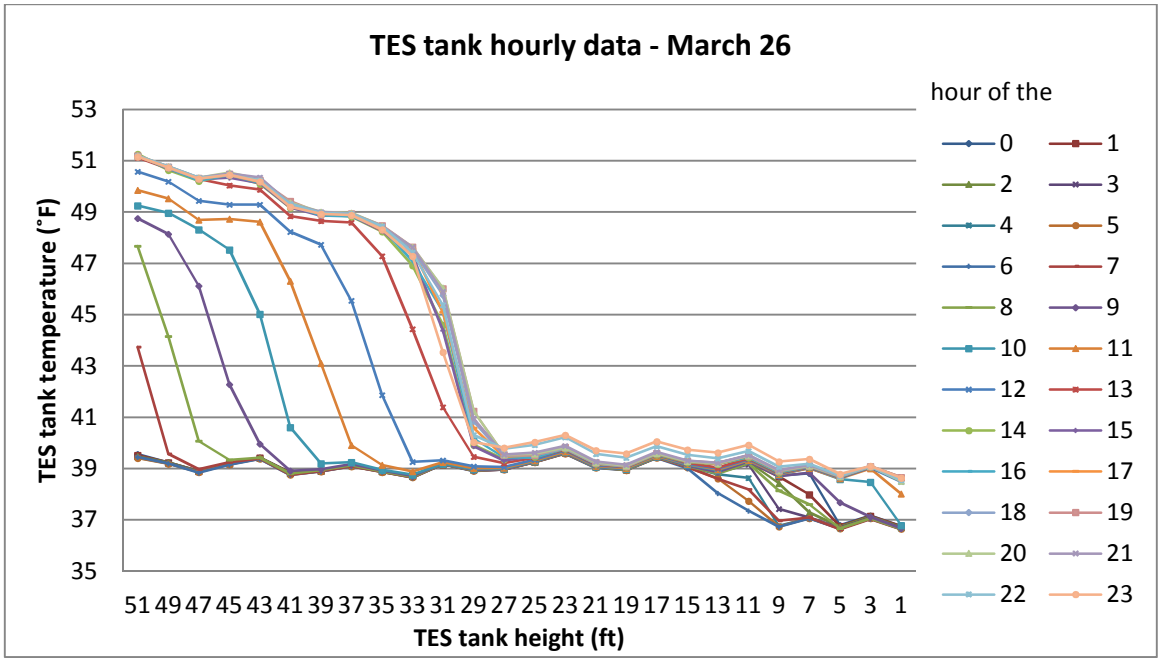

Figure 23. Hourly TES tank temperature data vs tank height for March 26, 2013

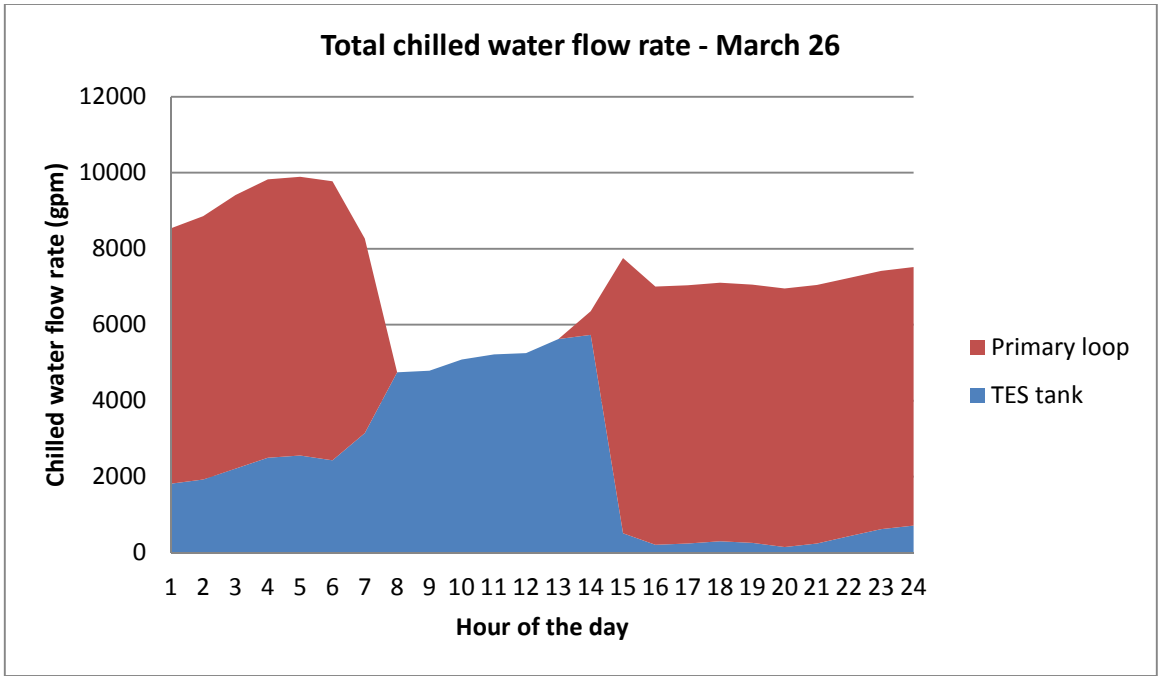

Figure 24. TES tank flow rate compared to the primary loop flow rate for March 26, 2013

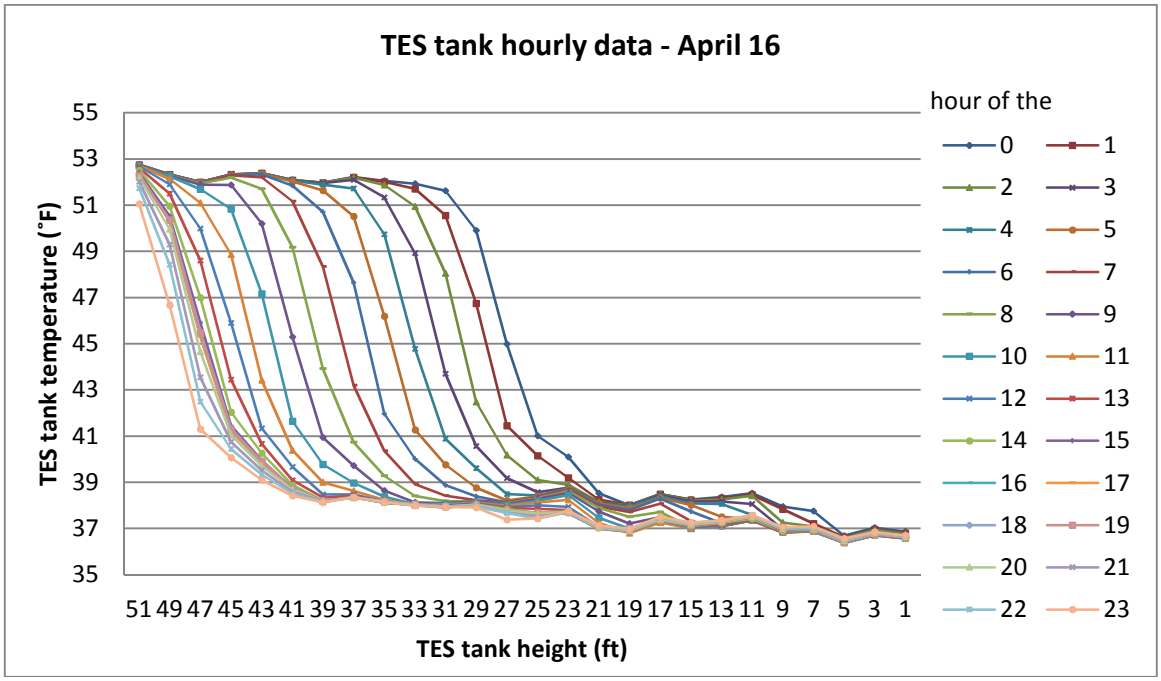

Figure 25. Hourly TES tank temperature data vs tank height for April 16, 2013

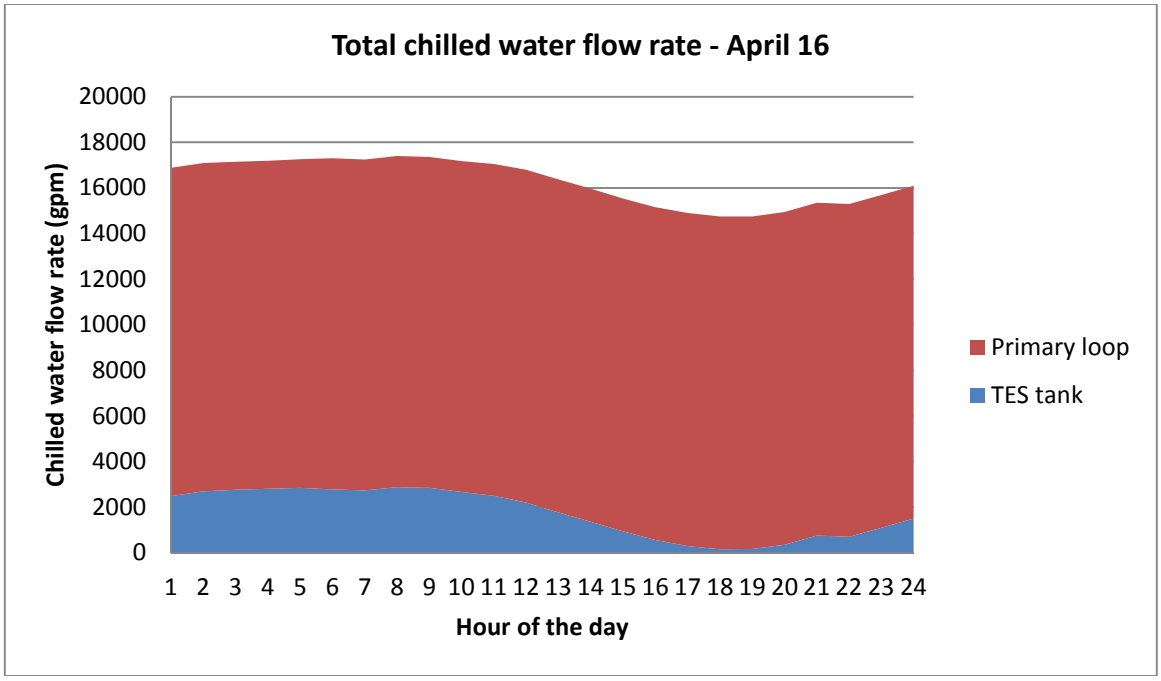

Figure 26. TES tank flow rate compared to the primary loop flow rate for April 16, 2013

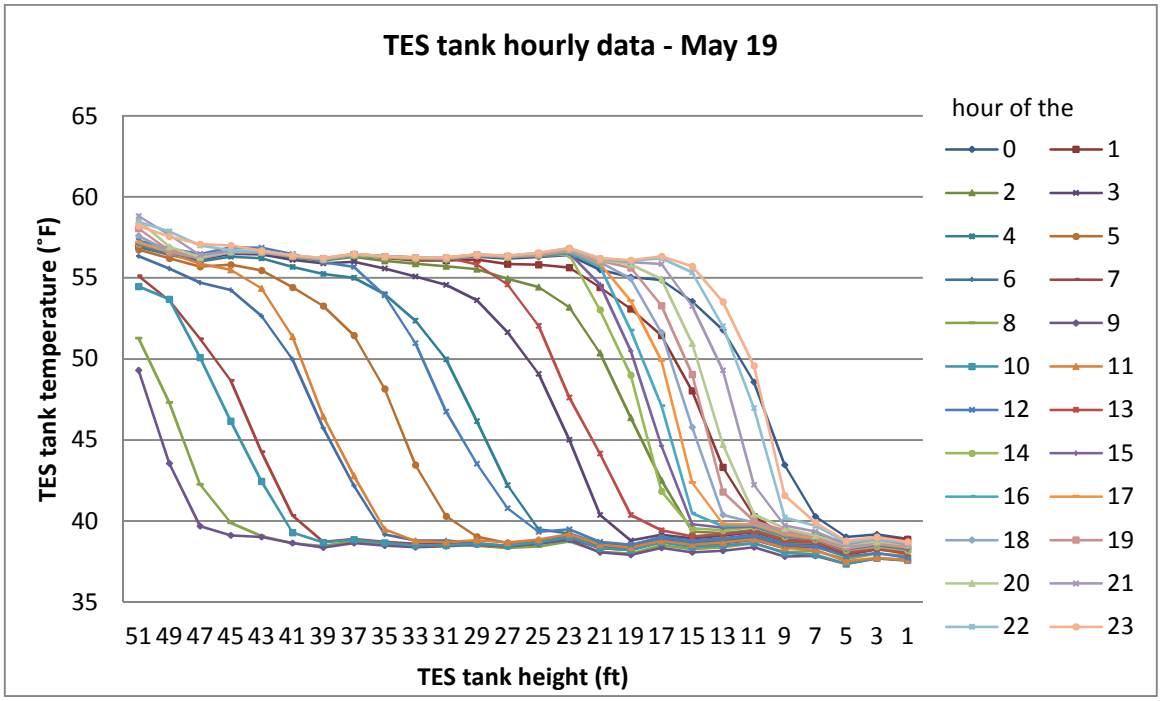

Figure 27. Hourly TES tank temperature data vs tank height for May 19, 2013

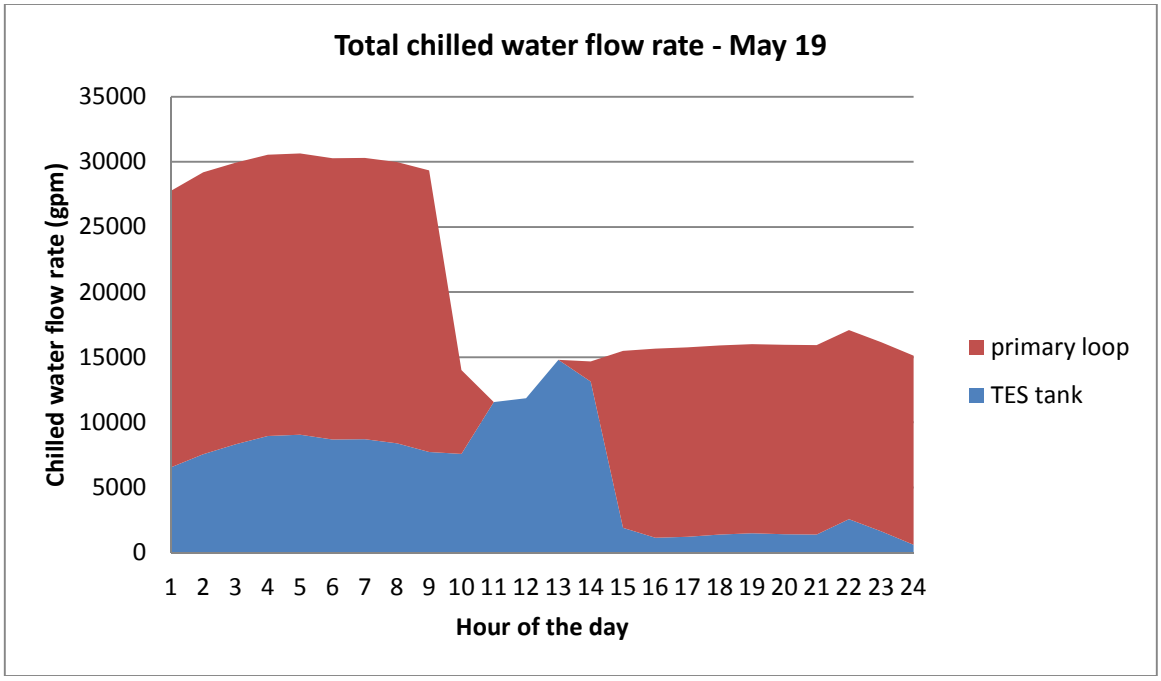

Figure 28. TES tank flow rate compared to the primary loop flow rate for May 19, 2013

Primary-Secondary system

Chilled water systems that work as primary-secondary variable flow systems, may present mixing of the return water with the supply water if the water flow from the primary loop is insufficient to meet the cooling loads. The mixing of return and supply chilled water would increase the ChWST and further worsen the problem. In the DFW Airport's plant, the primary loop and the TES tank discharge chilled water flow mix after the chiller discharge side header, before the secondary pumps suction side header. For that reason, the primary loop flow and TES tank flow are added together to investigate if mixing takes place in this chilled water plant.

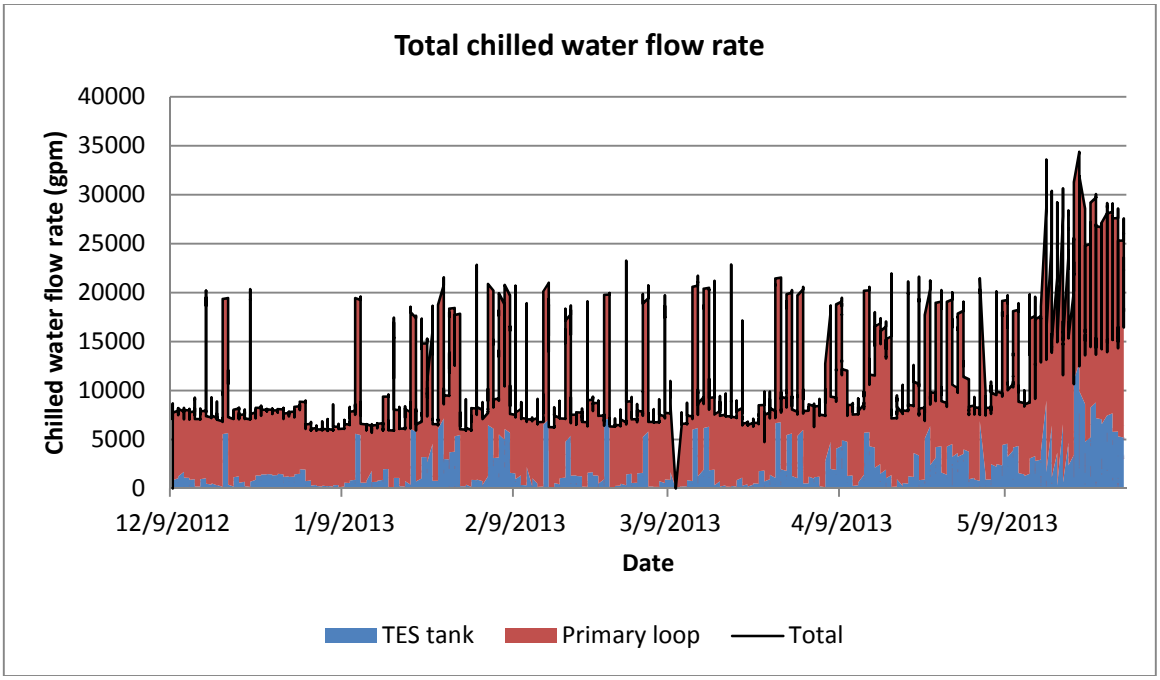

Figure 29. TES tank flow rate and primary loop flow rate for the DFW Airport's CUP

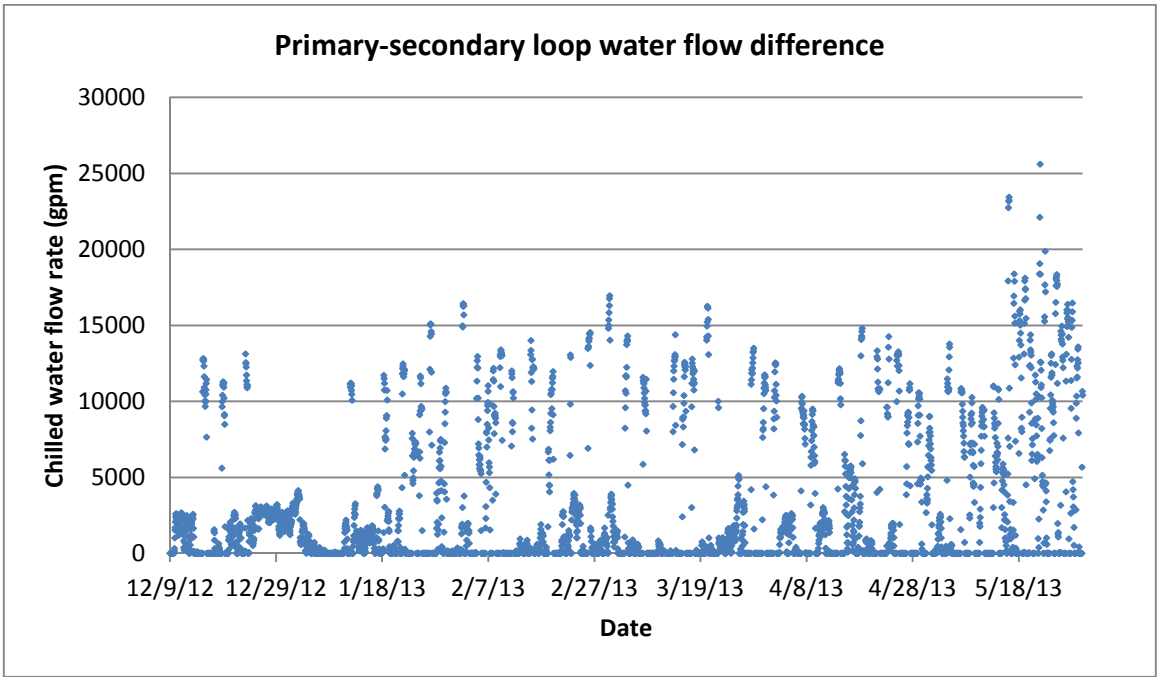

Figure 30. Primary loop minus secondary loop flow rate for the DFW Airport's CUP

As seen in figures 29 and 30, the secondary loop water flow is never larger than that of the primary loop and the TES tank discharge added together. Furthermore, the primary loop and TES tank water flow exceeds that of the secondary loop by at least 6,000 gpm slightly over 18% of the time from December 2012 to May 2013. Thus, there may be room for energy savings in the TES tank discharge management and chillers staging.

Chiller modeling

All 5 working chillers are simulated following the Gordon Ng model. They are regressed using data from January to December of 2013. The model accurately predicted the power consumption compared to the measured data for power consumption.

The constants $\Delta S_{int} Q_{eqv}^{leak}$ and R' where regressed for each chiller in the DFW Airport chilled water plant using equation 15. The data set used was measured from January 1st of 2013 to December 31st of 2013. The data corresponding to the periods where the chillers were on was used to perform the linear regressions.

After determining the regression constants $\Delta S_{int} Q_{eqv}^{leak}$ and R the predicted power is calculated using equation 17. It is important to notice that the temperatures must be entered in absolute units. In this study, the temperatures were entered in Rankine, the loads were entered in kBtu/hr and the condenser water flow in ft^3/hr.

Chiller 5 data showed that this chiller was never working during the time period studied. Thus, the study was performed on the 5 remaining chillers.

Figures 31, 32, 33, 34 and 35 show how the predicted power consumption properly correlates with measured power for all 5 working chillers.

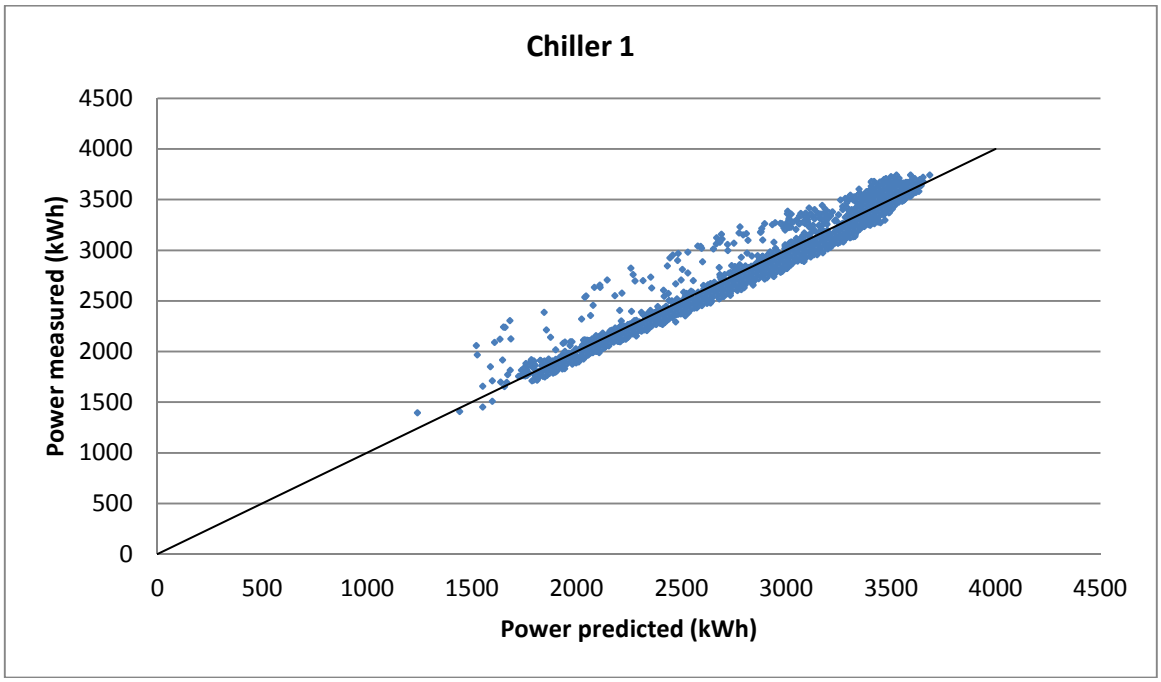

Figure 31. Predicted vs measured power for chiller 1

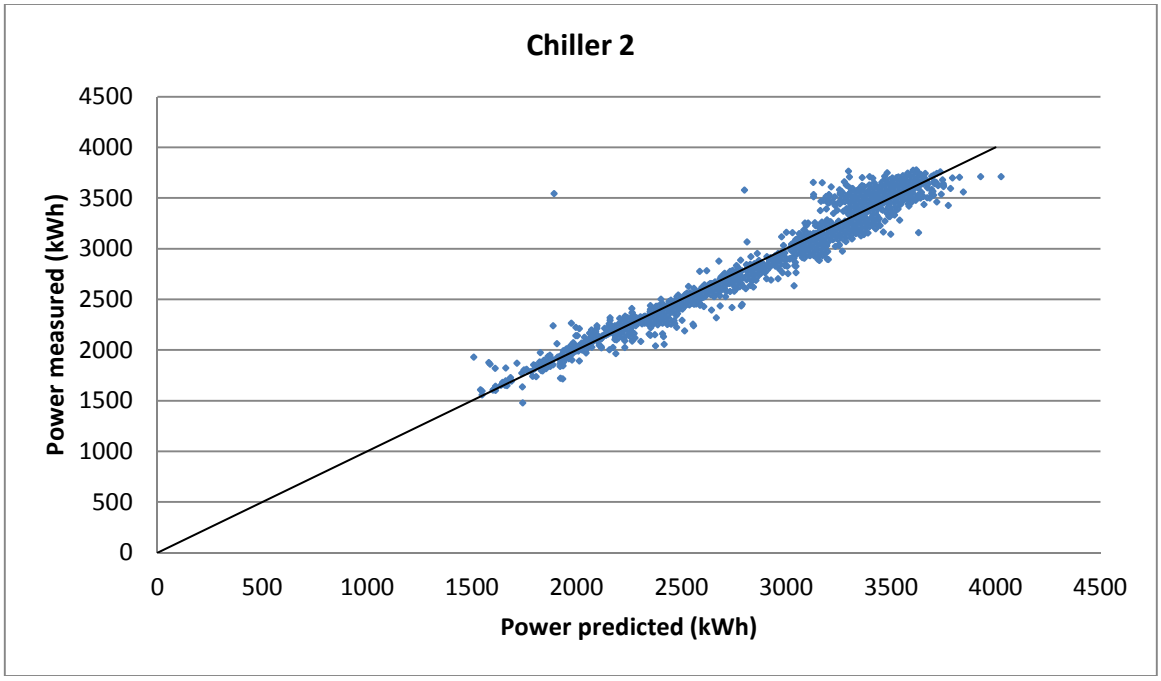

Figure 32. Predicted vs measured power for chiller 2

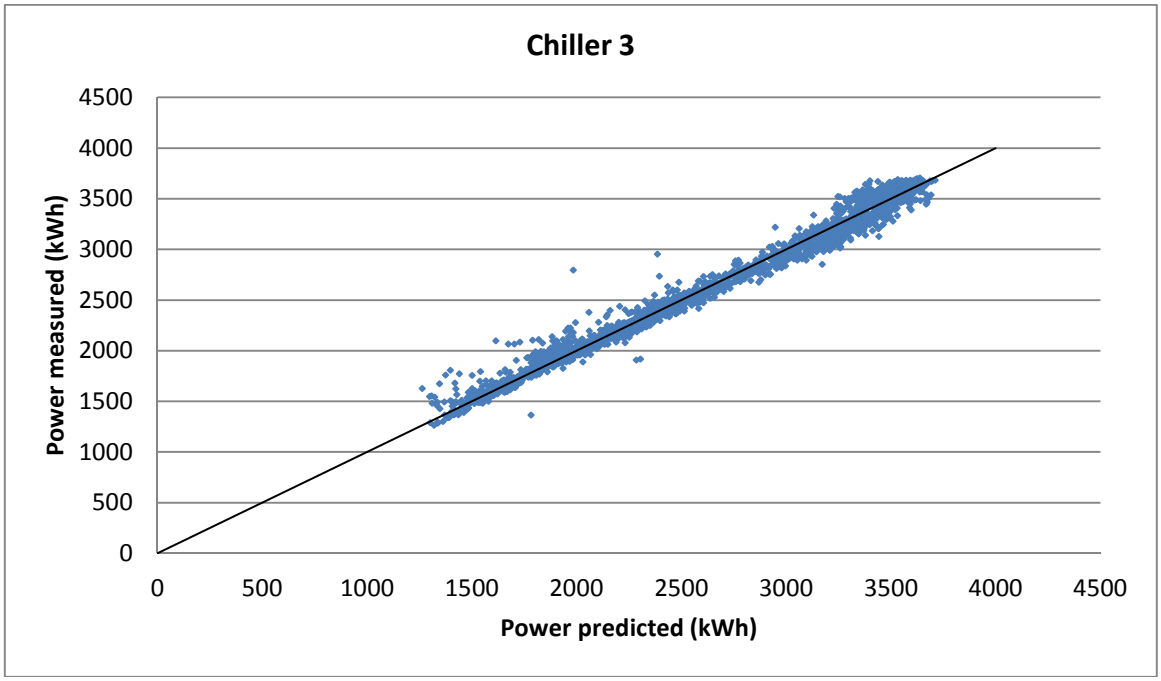

Figure 33. Predicted vs measured power for chiller 3

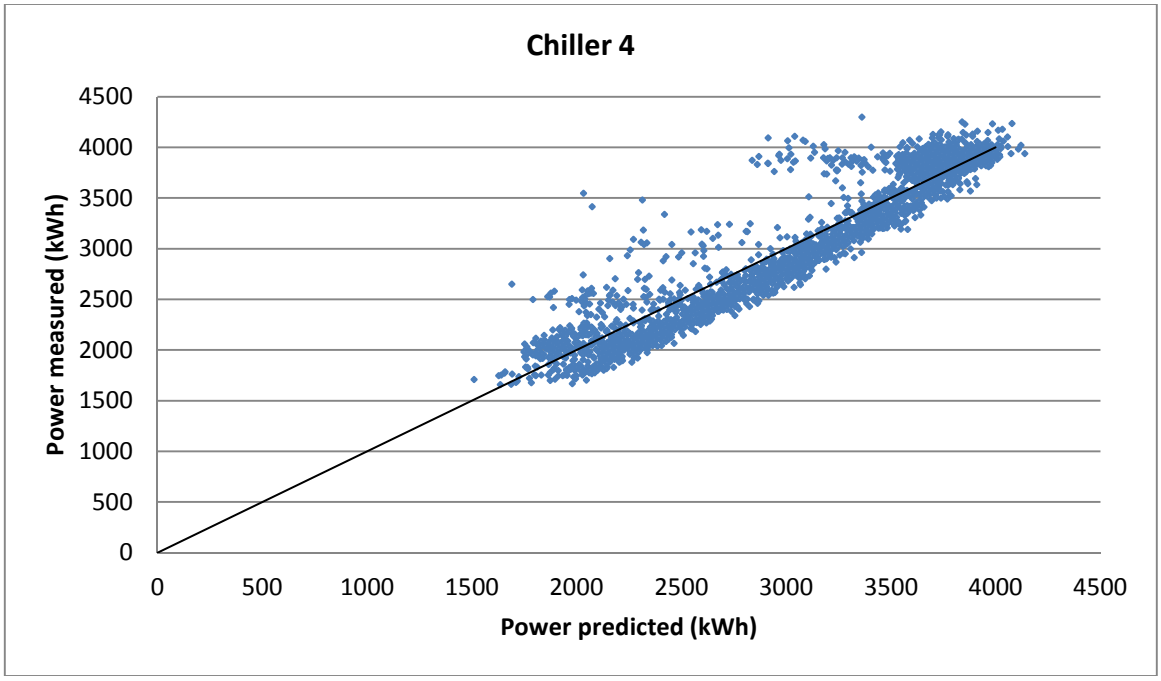

Figure 34. Predicted vs measured power for chiller 4

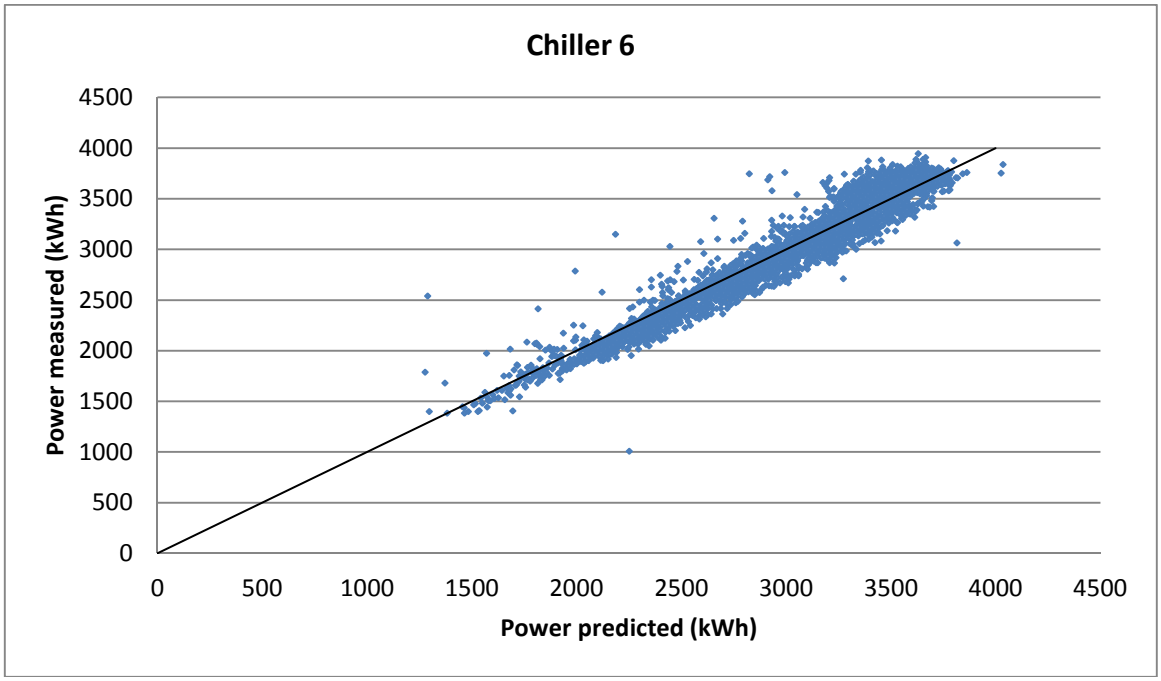

Figure 35. Predicted vs measured power for chiller 6

Parametric analysis

The chiller models are used to perform a parametric study, and predict the savings for each of the changes proposed.

After analyzing condenser temperature data, it was concluded that the cooling tower operation reset schedule was based on the outside air wet bulb temperature. Thus, the reset schedule proposed for this study maintains a 5˚F approach temperature whenever the wet bulb temperature is above 55˚F, and maintains a 60˚F cooling tower leaving temperature when the outside air temperature drops below 55˚F.

Figure 36 shows the approach and condenser water supply temperatures measured against outside air wet bulb temperature. As seen on the data the cooling tower has the capability to handle approach temperatures of 5˚ F, at points even go lower than 5˚F. Thus, maintaining a 5˚F approach should be feasible for the cooling towers operating at the DFW Airport.

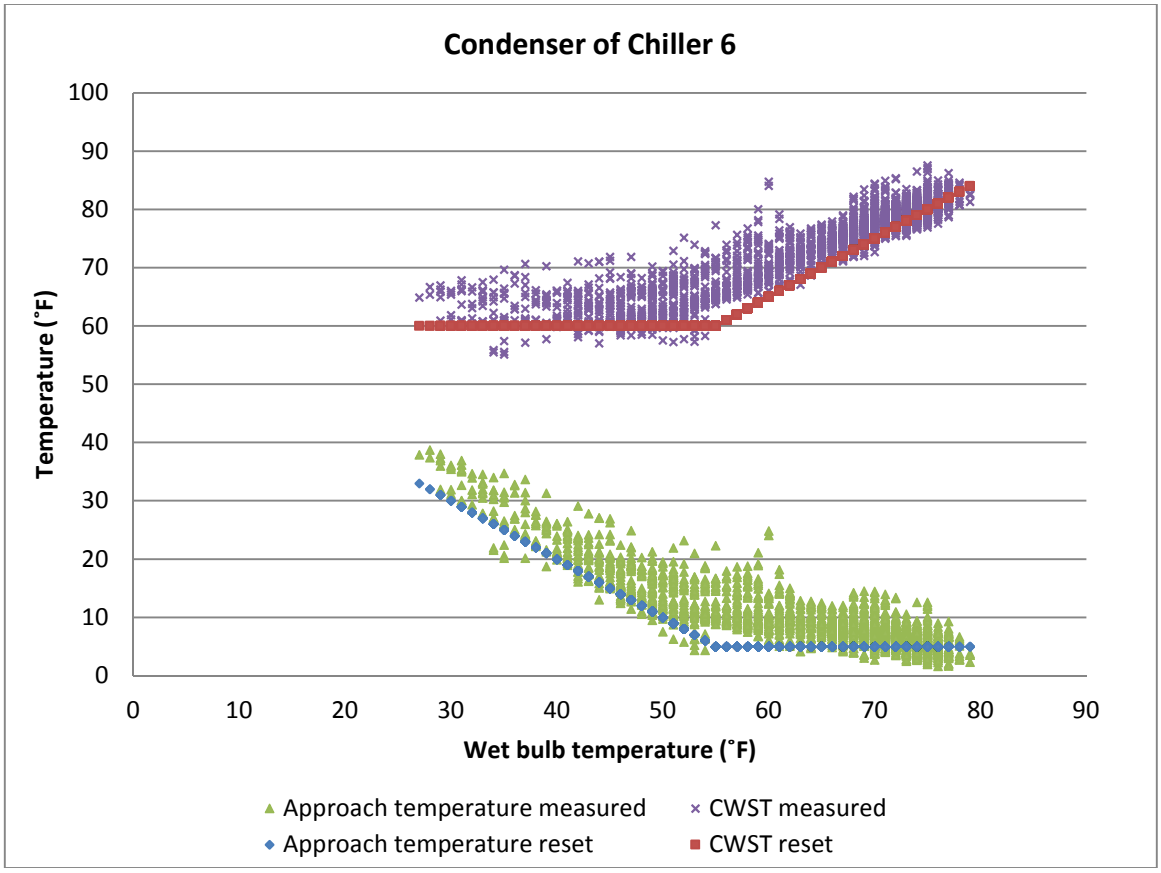

Figure 36. Condenser supply and approach temperature

The condenser water supply temperature (CWST) chiller model input is changed to maintain a 5˚F approach temperature if the outside air wet bulb temperature is above 55˚F. The CWST is maintained at 60˚F when the outside air wet bulb temperature drops below 55˚F.

The change in CWST yields savings in energy consumption for all 5 working chillers. The following plot shows the measured and predicted power for the new approach temperature reset.

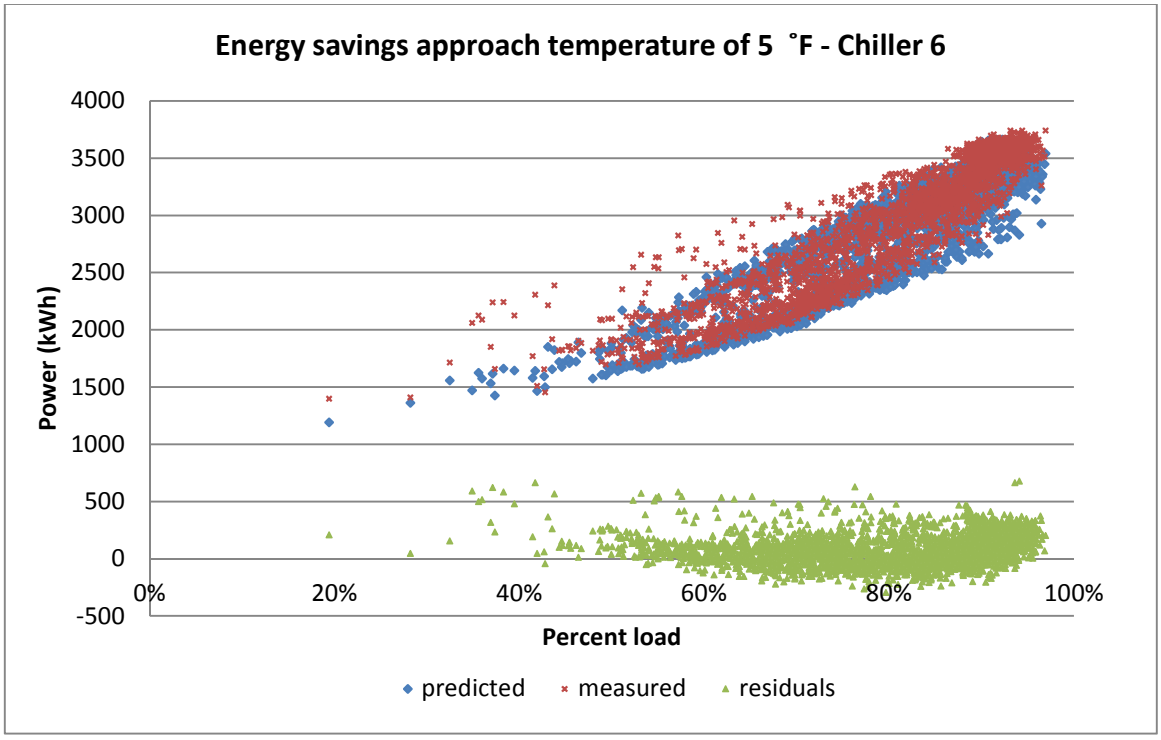

Figure 37. Energy savings for chiller 6 by changing the CWST

The residuals shown in figure 37 illustrate savings for most operating conditions. Even though the energy consumption predicted is higher than measured at some partial loads, total potential chiller energy savings are 1,414,981 kWh.

The next variable input modified in the chiller model was the ChWST. The simulation was carried out by varying this temperature from 36˚F to 44˚F increasing one degree at a time. The power consumption was plotted for 36˚F and 44˚F for all working chillers. Figure 38 shows the energy consumption of chiller 6 assuming a 5˚F approach temperature and 70,000 ft^3/hr condenser water flow. Chiller 6 is used to illustrate all working chillers behavior because it is the chiller that has the most hours of operation.

As seen in the results found in the chiller simulation, the chiller saved the most energy working at the highest possible ChWST under all load conditions as expected. It is important to note that the ability to charge the TES tank is not yet considered.

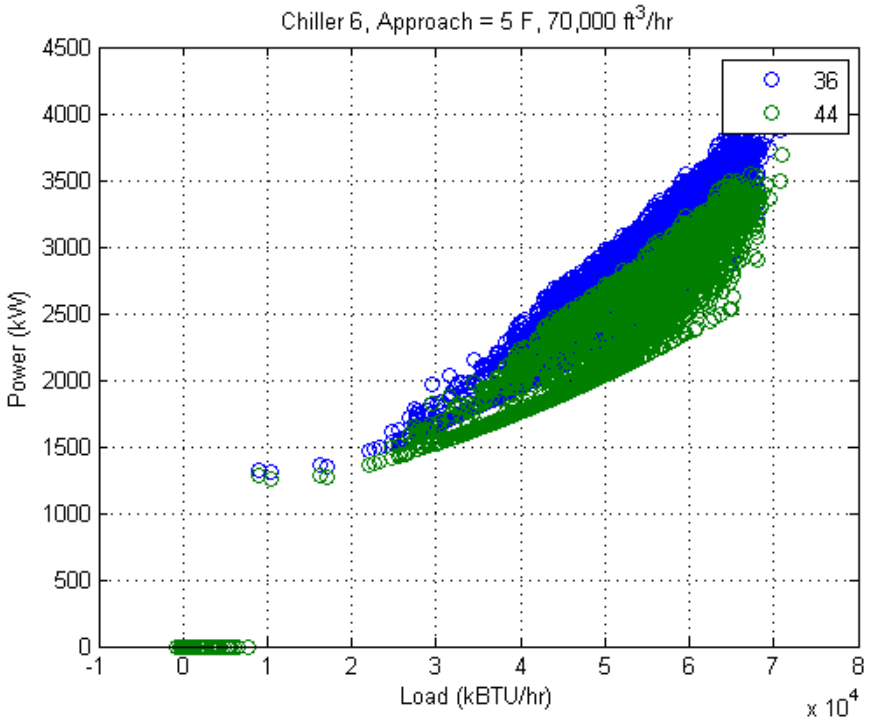

Figure 38. Predicted power consumption with an approach temperature of 5˚F, a condenser water flow of 70,000 ft^3/h with a ChWST of 36˚F and 44˚F

The last optimized variable was the condenser water flow. This variable range was decided based on condenser water pumps current operation and pumping capacity. The condenser flow was varied to 50,000 ft^3/hr (~6,230 gpm), 70,000 ft^3/hr (~8,730 gpm) and 100,000 ft^3/hr (~12,465 gpm). Figures 39 and 40 shows the energy consumption of chiller 6 maintaining both 36˚F and 44˚F ChWST, and 5˚F approach

temperature. In both scenarios, chiller energy savings were largest when the condenser water is kept at 100,000 ft^3/hr (~12,465 gpm). The additional pumping power at higher flow rates was not considered in this analysis since no measured condenser water pumping power is available.

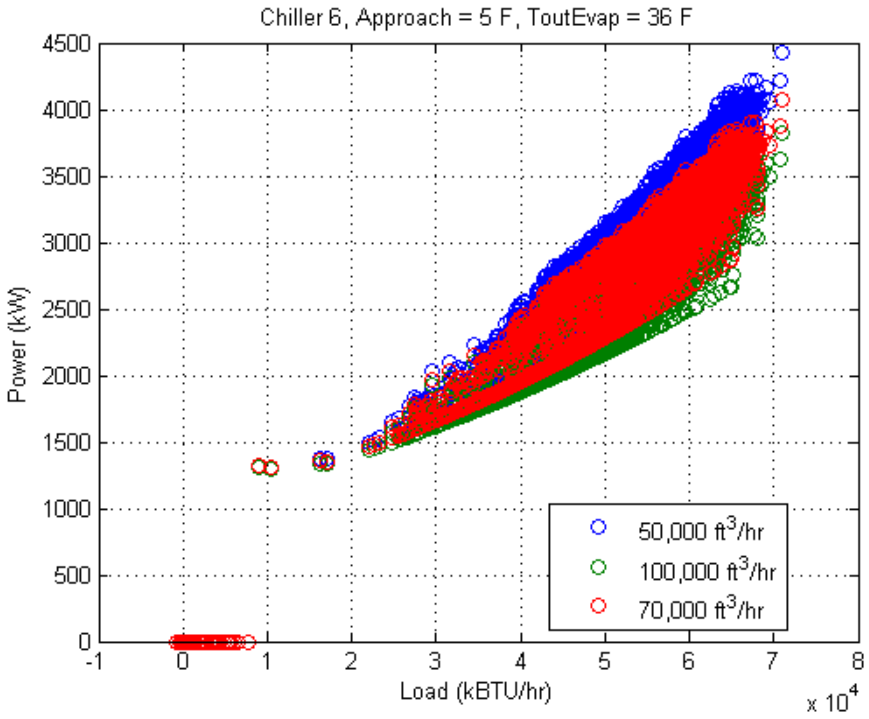

Figure 39. Predicted power consumption with an approach temperature of 5˚F, ChWST of 36˚F and a condenser water flow of 70,000 ft^3/h

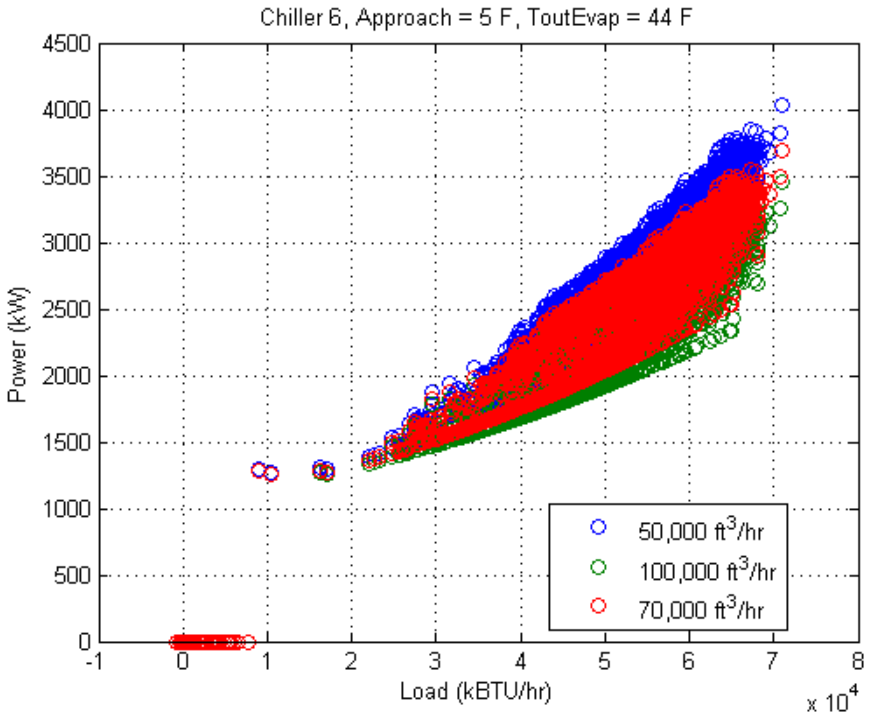

Figure 40. Predicted power consumption with an approach temperature of 5˚F, ChWST of 44˚F and a condenser water flow of 70,000 ft^3/h

The condition for the largest chiller energy savings was evaluated by considering the results of the chiller simulation parametric analysis and was achieved under the following conditions:

- Maintaining a 5˚F approach temperature whenever the outside air wet bulb temperature is above 55˚F and maintaining a .60˚F CWST, whenever the outside air wet bulb temperature is below 55˚F.
- Maintaining the highest possible ChWST year round that would allow meeting the cooling loads and charging the TES tank.

- Running the condenser at 100,000 ft^3/hr (~12,465 gpm) per working chiller, year round.

The chiller simulation is used to predict the energy saved by running the chillers and cooling towers under new, optimized, conditions. Figure 41 shows the simulated chiller energy consumption, the current energy consumption, and the predicted energy savings for chiller 6.

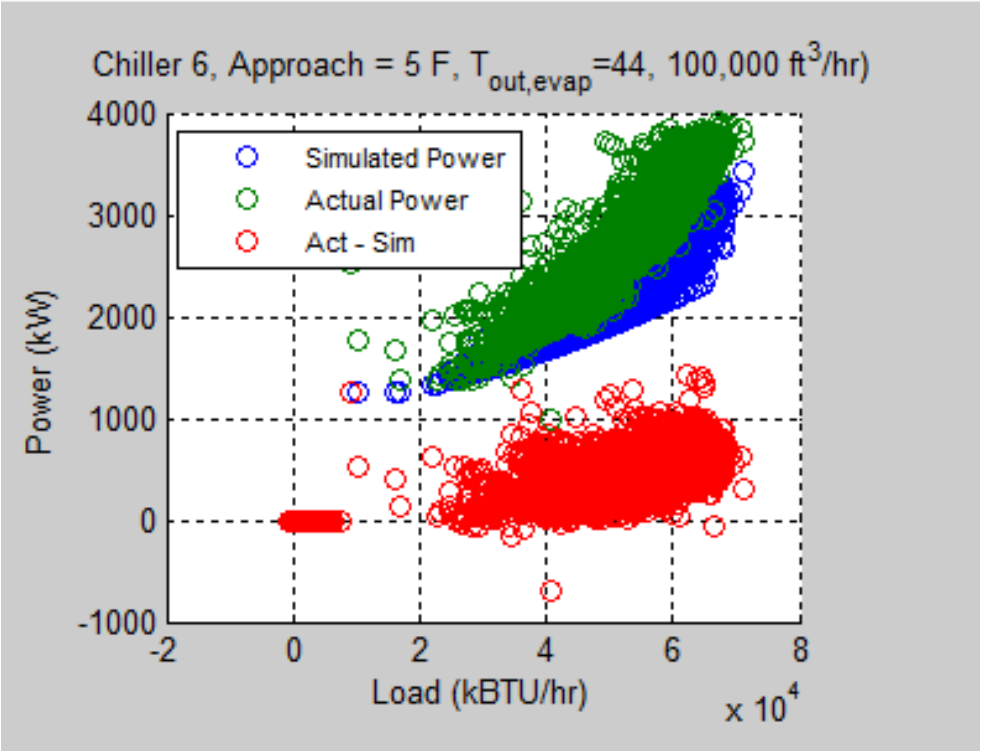

Figure 41. Measured and predicted power consumption with an approach temperature of 5˚F, ChWST of 44˚F and a condenser water flow of 70,000 ft^3/h. The residuals show the energy savings that the setpoint changes would yield.

The secondary pumps' new pumping power has been calculated to predict net energy savings. Due to lack of available data, it was not possible to calculate the new condenser pumps pumping power. However, it is important to consider that to obtain a more accurate result of energy savings this new pumping power has to be calculated.

It is also important to note that there is a rise of about 2˚F in the chilled water temperature from the CUP to the farthest building. This temperature rise was noticed after analyzing detailed data from the 2010 ESL study of the CUP, terminals, and buildings. This means that some buildings would receive chilled water at 46˚F. Since there is no theoretical way to determine whether the new ChWST would meet the air dehumidification required to maintain comfort and supply air temperature, it is advised, as a future study, to conduct tests in the DFW Airport with the proposed setpoints to ensure efficient operation.

Secondary loop delta-T model

The new secondary pumps' pumping power was calculated in order to estimate net energy savings. A regression model was built to predict the plant secondary loop delta-T. This delta-T is used to calculate the secondary pumps' new pumping power. This model was regressed from three variables: outside air wet bulb temperature, the plant load and ChWST. The ChWST setpoint was changed to 44˚F and the simulation was run with the measured data of cooling load and outside air wet bulb temperature for the current operations. This predicted delta-T was used in equation 26 to calculate the new water flow needed to meet the loads.

$$Q = \dot{m} C_p \Delta T$$

Equation 25

$$Q\left(\frac{Btu}{h}\right) = 500\ GPM\ \Delta T$$

Equation 26

Figure 42 shows the predicted water flow compared to the measured water flow.

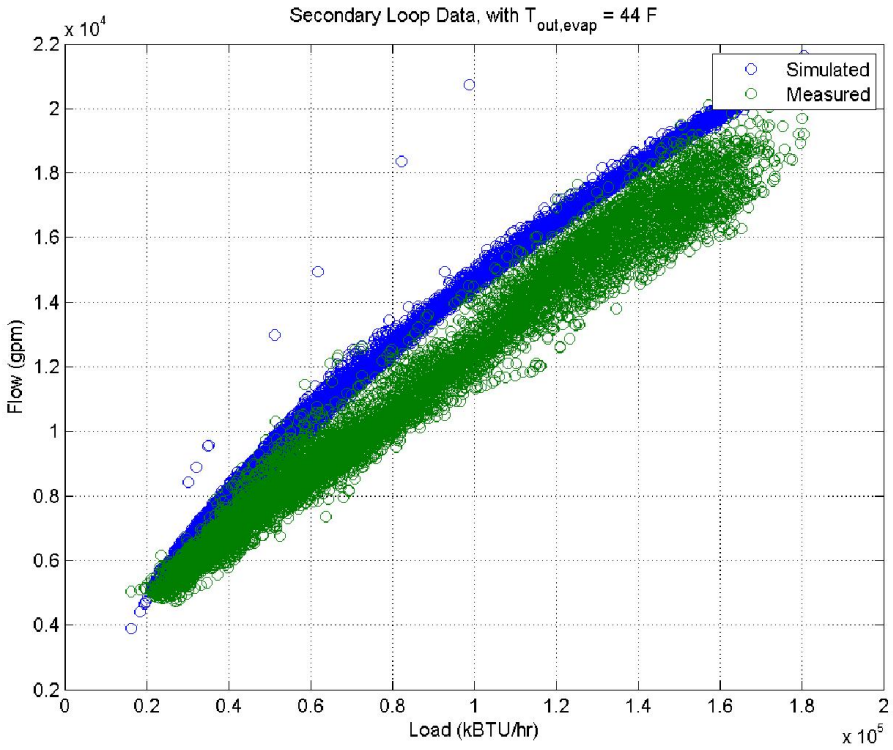

Figure 42. Measured water flow in the secondary loop and the predicted water flow required to meet the cooling loads with the new ChWST setpoint of 44˚F

The predicted power usage for the secondary pumps was calculated using the relationship presented in the CUP study performed by the ESL. This equation predicts the energy consumption based solely on water flow in the following way:

$$\text{Pump power (kW)} = 0.00000128(\text{ChW flow})^2 + 0.0007(\text{ChW flow}) + 24.024$$

Equation 27

The additional water needed to meet the loads under the new working conditions (44˚F for the ChWST) requires additional pumping power. Figure 43 illustrates the chiller energy savings compared to the additional energy required by the secondary pumps. It can be seen that chiller savings are significantly higher than the additional power required by the secondary pumps. Moreover, the energy savings depended mostly on the chiller staging and chiller energy consumption.

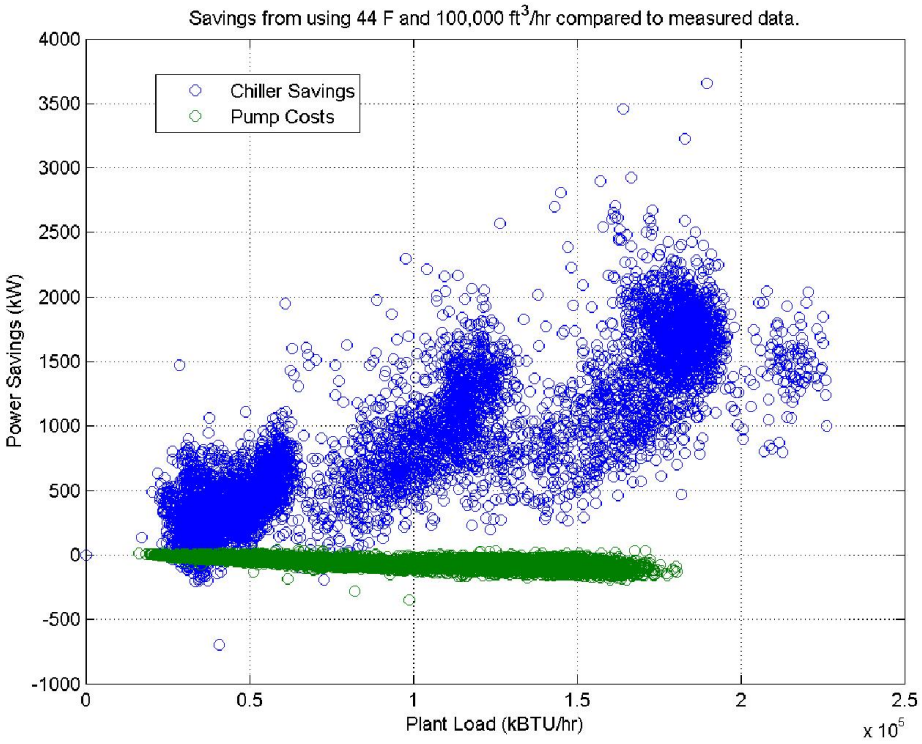

Figure 43. Total chiller energy consumption savings and the extra power needed by the secondary pumps due the rise in the secondary loop water flow

TES tank behavior

The TES tank is an essential part of the chilled water system in the DFW Airport. Thus, it is necessary to maintain enough chilled water in the tank to meet the airport's cooling loads. The tank data provided by the airport shows water temperature measurements every three feet of the tank's height. With this data, it was possible to verify the height and volume of chilled water present in the tank. Figure 44 illustrates the chilled water level in the tank for the period from January 2013 to May 2013.

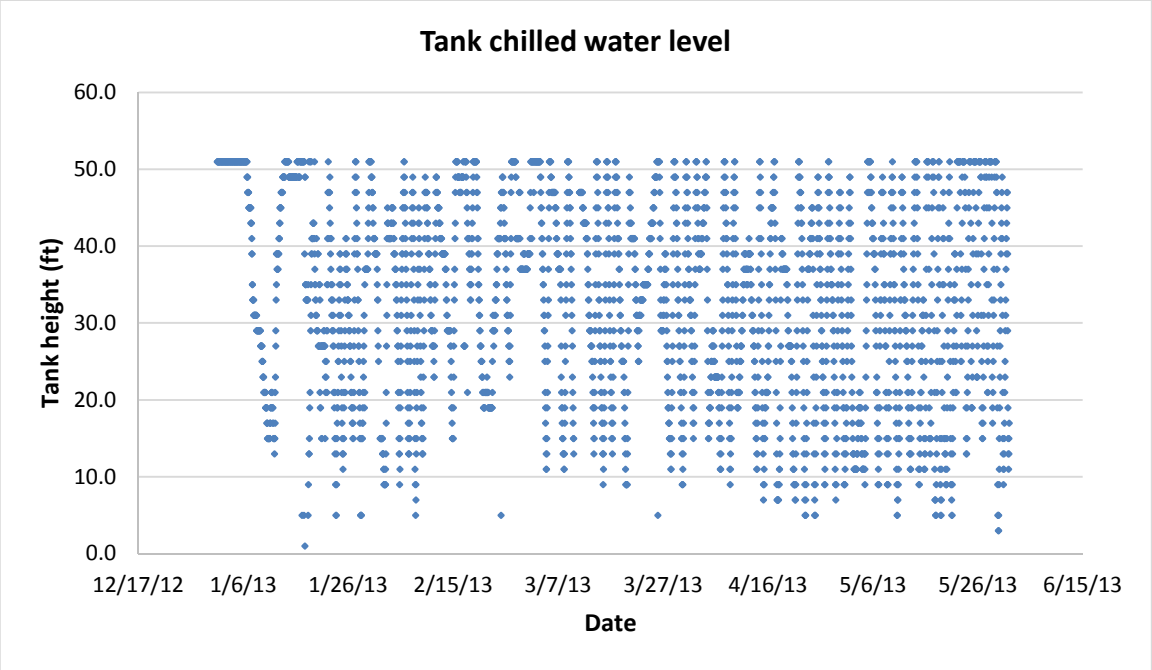

Figure 44. Measured chilled water level on the TES tank

The chilled water ratio is calculated from primary and secondary loop measured data. The chilled water ratio of 1 represents the tank full of chilled water, and 0 represents the tank has no chilled water. The chilled water ratio calculated with equation 22 is compared to the chilled water level measured in the tank to ensure that the calculated chilled water ratio corresponds to measured data. Figure 45 shows the chilled water ratio for current operation:

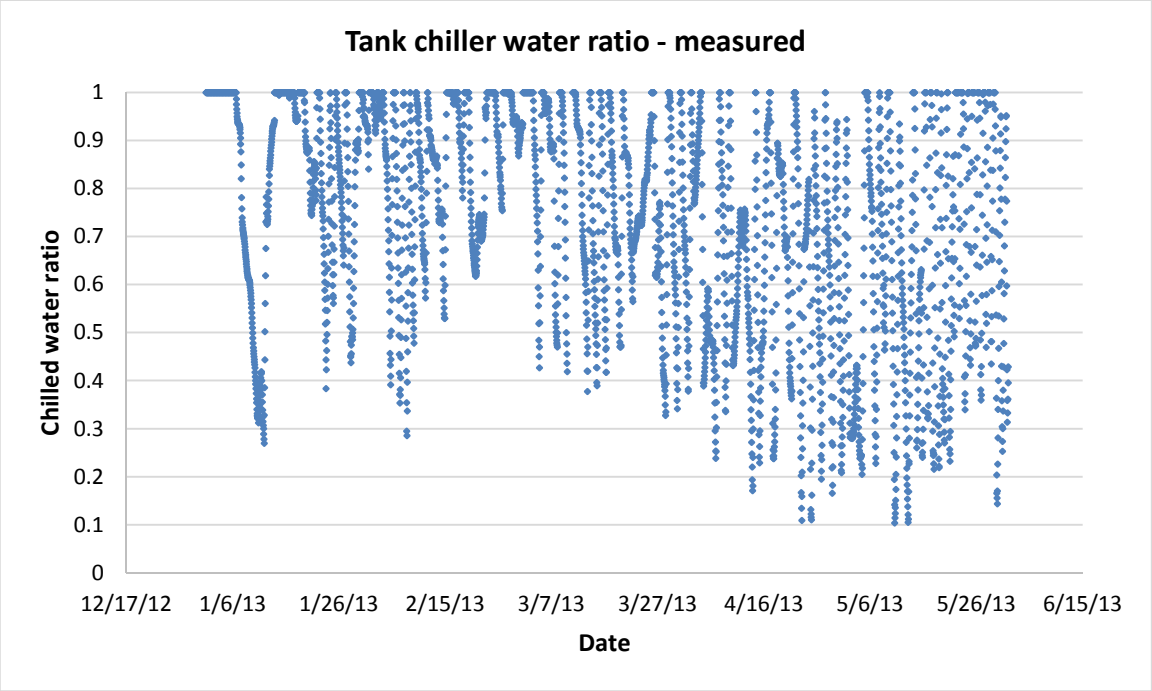

Figure 45. TES tank chilled water ratio calculated with measured data

After confirming that the tank chilled water level and ratio followed the same trend, the chilled water ratio tank model was carried out with the variable's new setpoints found in the optimization process.

According to the results given by the tank simulation, the 44˚F ChWST provided by the same number of chillers currently working is not enough to meet the loads and fill the TES tank with sufficient chilled water. The secondary loop water flow increase due to the ChWST setpoint of 44˚F, makes the primary water flow insufficient to fill out the tank with the required chilled water level. As seen in figure 46, the tank consistently runs out of chilled water throughout the period of measured data. Consequently, the tank

would provide water at the return temperature to the secondary loop and the system would be unable to meet the cooling loads.

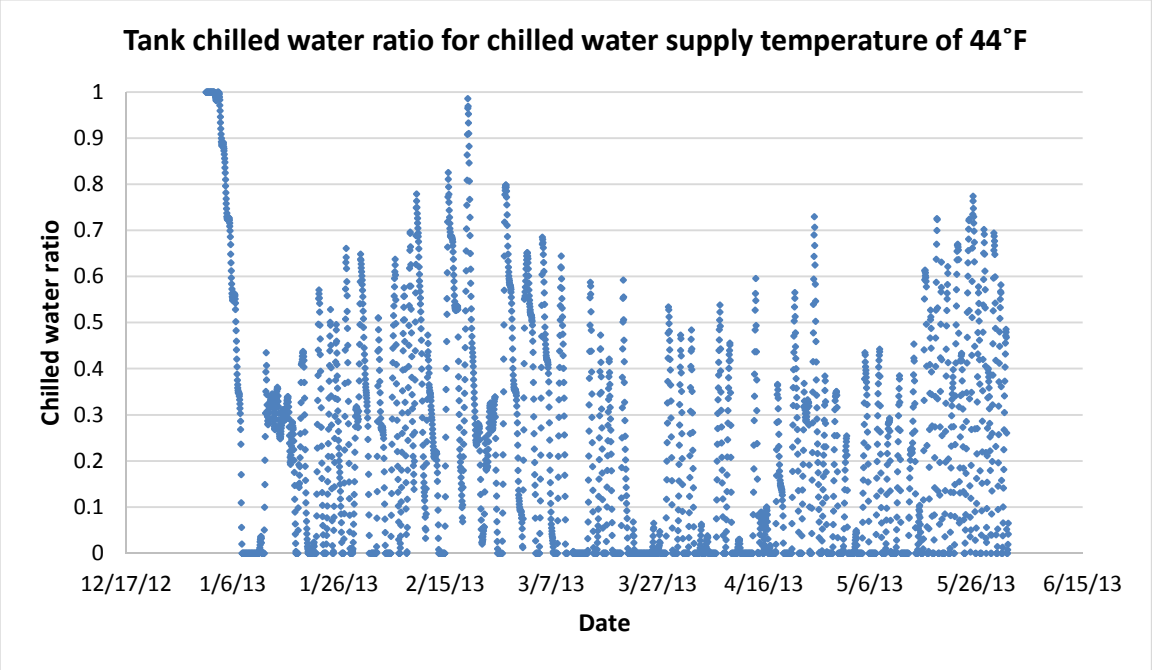

Figure 46. TES tank chilled water ratio predicted for a ChWST of 44˚F

The ChWST setpoint was changed to 42˚F. This new ChWST setpoint was sufficient to maintain enough chilled water in the tank for the months of January and February. As presented in figure 47.

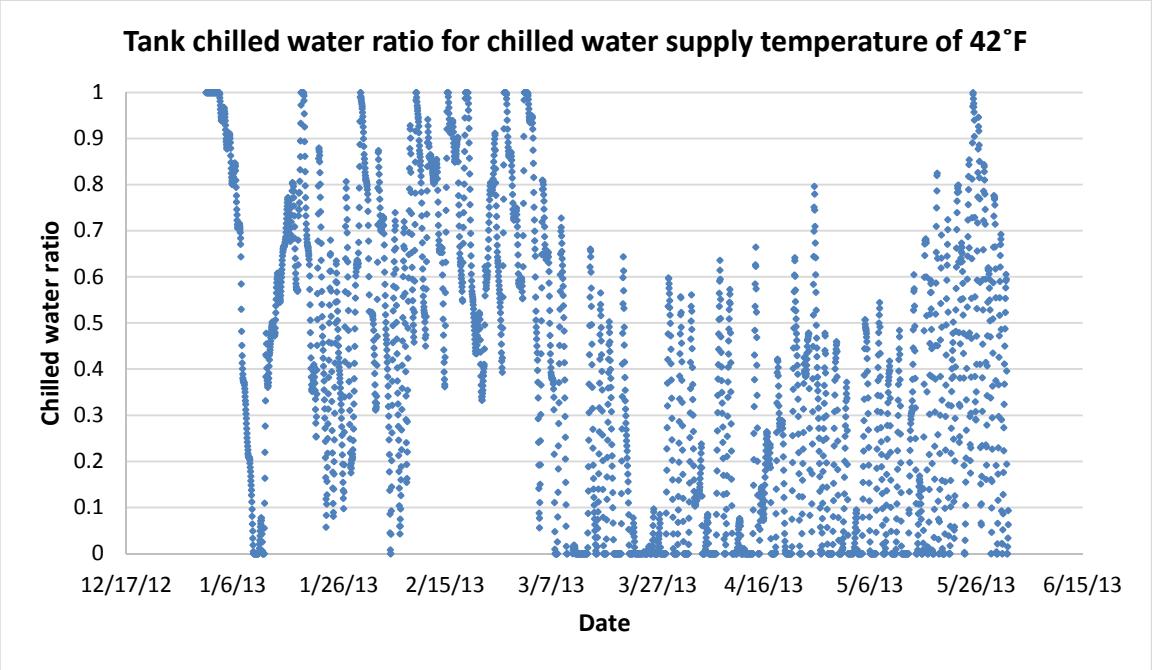

Figure 47. TES tank chilled water ratio predicted for a ChWST of 42˚F

Then, the chilled water level in the tank was studied under different ChWST setpoints, concluding that keeping a 42˚F ChWST in the months of January and February maintains enough chilled water in the tank to meet the airport cooling loads. During the moths of March, April and May, the ChWST setpoint was decreased to 37˚F, which was sufficient to meet the airport cooling loads and the required tank chilled water level. Figure 48 shows the TES chilled water ratio following the ChWST reset schedule of 42˚F for the months of January and February and 37˚F for the moths of March, April and May.

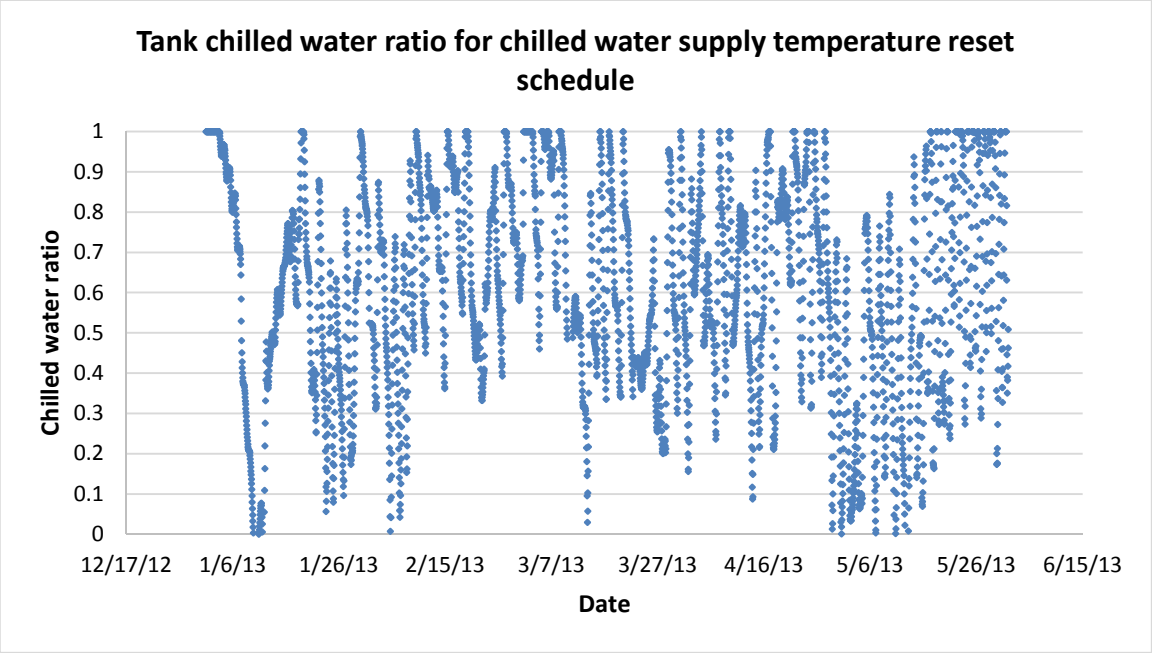

Figure 48. TES tank chilled water ratio predicted for a ChWST of 44˚F

Since there was no tank data available after May 31st 2013, the reset schedule was extended to the rest of the year based on outside air temperature monthly schedule. The ChWST of 37˚F is extended to the months of June through October, and for the month of November and December is changed to 42˚F. The energy savings were recalculated using the new reset schedule for the ChWST.

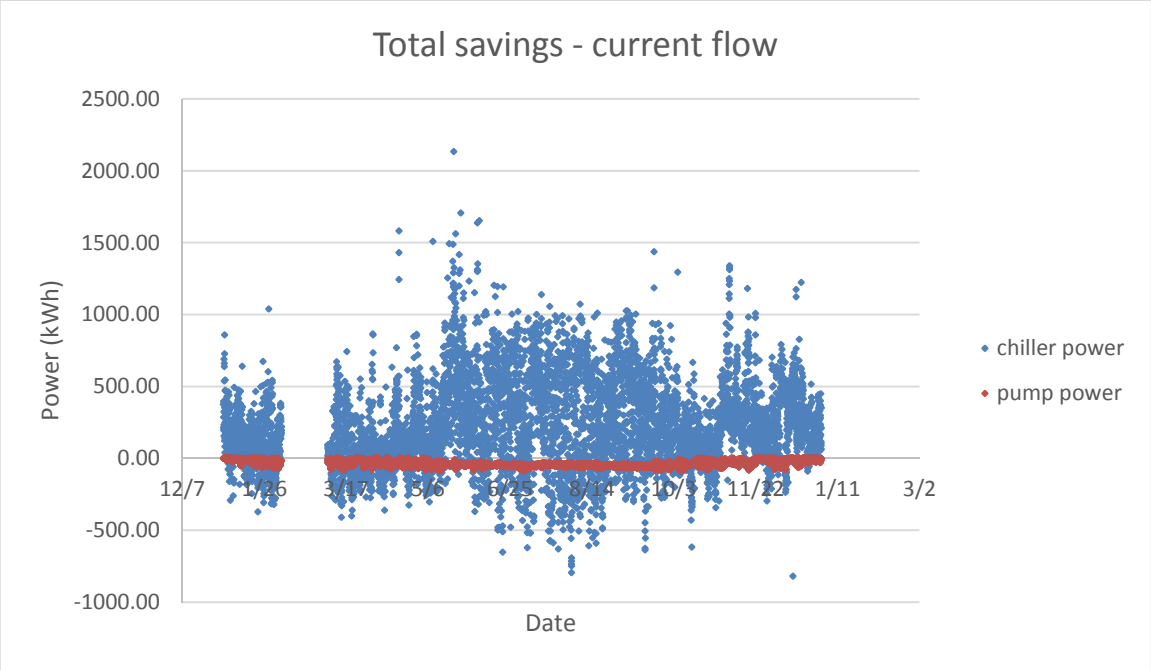

Figure 49. Total energy savings under the proposed reset schedule for the ChWST and CWST. However, the condenser water flow is maintained as current operation.

Figure 49 shows predicted power consumption under the ChWST reset schedule of 42˚F for January and February, 37˚F for the months of march through October and back to 42˚F for November and December. The CWST has no impact on the tank chilled water level, so its reset schedule is maintained at 5˚F approach temperature whenever the wet bulb temperature is above 55˚F, and 60˚F cooling tower leaving temperature when the outside air temperature drops below 55˚F. The condenser water is maintained at current operation because there is no way to predict the additional energy required by the condenser pumps to run the additional condenser water. The total energy savings calculated were 1,588,813 kWh, which represents 3.81% savings.

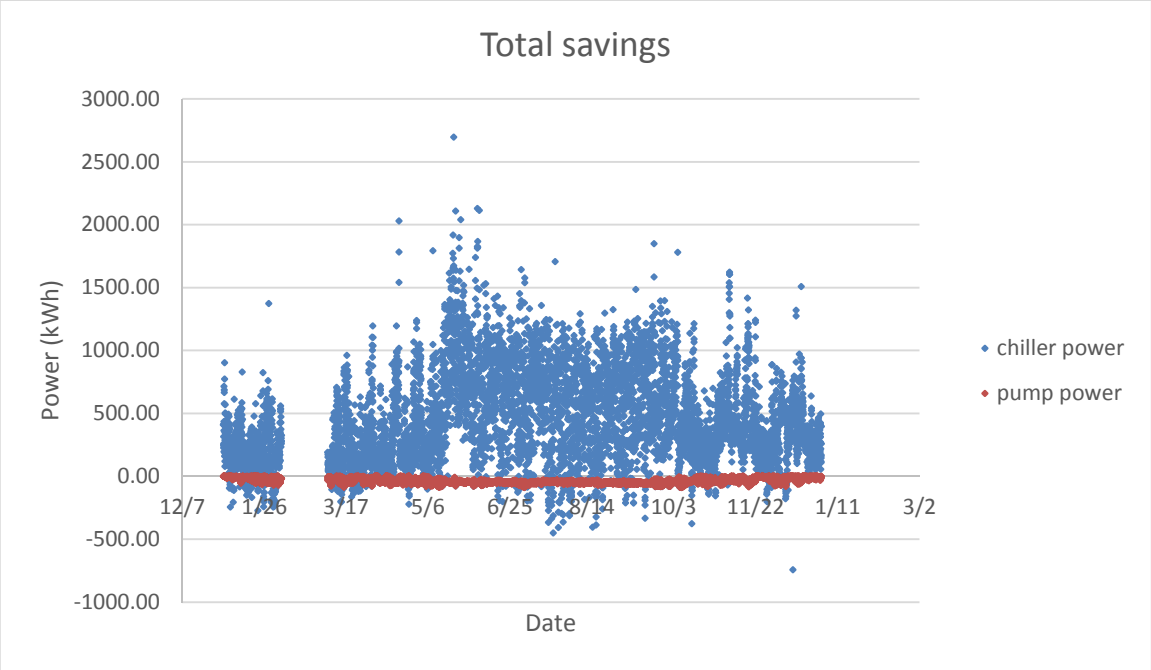

Figure 50.Total energy savings under the proposed reset schedule for the ChWST, CWST and condenser water flow rate.

The energy savings were also calculated when the condenser water is maintained at 100,000 ft^3/h year round. Figure 50 shows the predicted savings under these conditions. However, these are not net savings, because it is not possible to predict the required additional condenser pumping power. The total chiller energy savings calculated were 3,237,402 kWh, which represents 7.76% savings.

CHAPTER V

CONCLUSIONS AND FUTURE WORK

Conclusions

The chilled water system at the DFW Airport has a primary and secondary loop and is comprised of 6 chillers, 8 cooling towers and a TES tank. The system's data was analyzed and models for the chillers, cooling towers and TES tank chilled water level were built. After running the simulations for the chillers, it was concluded the chillers worked more efficiently with higher ChWST. Also, the most energy savings were achieved when the condenser water ran the highest water flow, that is 100,000 ft^3/hr (~12,465 gpm) per working chiller, year round. The condenser water supply temperature reset schedule was to maintain a 5˚F approach temperature whenever the outside air wet bulb temperature is above 55˚F and maintaining a 60˚F condenser water supply temperature, whenever the outside air wet bulb temperature is below 55˚F.

The TES tank simulation is used to determine the ChWST that would improve chiller performance while meeting the cooling loads and properly charging the TES tank. According to the results of the TES tank simulation, the optimum ChWST reset schedule was 42˚F for the months of January and February, 37˚F from March through October, and back to 42˚F for the months of November and December. Due to the rate schedule, the chillers are switched off and the tank provides all the chilled water for the DFW Airport from 3pm to 6 pm for the months of June through September. Thus, it is important to maintain the required chilled water level in the tank at all times.

The chillers and secondary pumps power consumption was predicted using the chiller and secondary pumps models. The simulations were run using the proposed reset schedules, that is, a ChWST reset schedule of 42˚F for the months of January and February, 37˚F from March through October, and back to 42˚F for the months of November and December. The CW supply temperature was maintained with a 5˚F approach temperature whenever the outside air wet bulb temperature is above 55˚F and a 60˚F condenser water supply temperature, whenever the outside air wet bulb temperature is below 55˚F. Due to lack of condenser water data, it was not possible to simulate condenser water pumping power. For this reason, the simulation was initially run using current operation condenser water flow. The total energy savings predicted were 1,588,813 kWh, which represents 3.81% savings. Subsequently, the chiller simulation was run using also the condenser water flow rate of 100,000 ft^3/hr (~12,465 gpm) per working chiller, year round. The predicted energy savings were 3,237,402 kWh, which represents 7.76% savings. However, the additional power required by the condenser pumps is not taken into account. Thus, the predicted energy savings calculated with a condenser water flow rate of 100,000 ft^3/hr (~12,465 gpm) per working chiller, year round are not net savings.

Future work

To calculate the net savings yielded by the new proposed reset schedules, it is very important to calculate the additional power consumed by the condenser pumps. This thesis does not include a model for the condenser pumps due to lack of available

data. It is suggested to obtain the necessary data to build a model for the condenser pumps to predict net savings.

It is also advised to record data on the cooling towers fans to determine the impact of running additional water on the cooling towers on the fan performance.

Finally, it is recommended to test the proposed reset schedules on the DFW airport chilled water plant to ensure that the cooling loads are met and the space is comfortably maintained.

REFERENCES

(EIA), E. I. A. (2014). from http://www.eia.gov/beta/MER/?tbl=T02.01#/?f=M. Energy consumption by sector.

(ESL). (2011). Dallas/Fort Worth International Airport (DFW) Central Utility Plant Hydraulic Systems Analysis: 27-30

Ahn, B. ; Mitchell, J. (2001). "Optimal control development for chilled water plants using a quadratic representation." Energy and Buildings **33**(4): 371-378.

American Society of Heating, Refrigeration and Air-Conditioning Engineers, Inc. (2004). Ashrae Handbook. Hvac Systems and Equipment. Atlanta, GA.

Avery, G. (2001). "Improving the Efficiency of Chilled Water Plants." Ashrae **43**(5): 14-18.

Çengel, Y.; Boles, M. (2006). Thermodynamics : an engineering approach. Boston, McGraw-Hill Higher Education

Braun, J.; Klein, S.; Mitchell, J. (1989). "Effectiveness models for cooling towers and cooling coils." Ashrae Transactions **96**(2): 164-174.

Cortinovis, G. ; Paiva, J. ; Song, T. ; Pinto, J. (2009). "A systematic approach for optimal cooling tower operation." Energy Conversion and Management **50**(9): 2200-2209.

Cortinovis, G. ; Ribeiro, M. ; Paiva, J. ; Song, T. ; Pinto, J. (2009). "Integrated analysis of cooling water systems: Modeling and experimental validation." Applied Thermal Engineering **29**(14-15): 3124-3131.

Figueroa, I.; Medina, M.; Cathey, M.; Nutter, D. (1998). Predicting improved chiller performance through thermodynamic modeling. Industrial Energy Technology Conference, Houston, Texas.

Fiorino, D. (1999). "Achieving High Chilled-Water Delta Ts." Ashrae **41**(11): 24-30.

Gao, D.; Wang, S.; Sun, Y. (2011). "A fault-tolerant and energy efficient control strategy for primary-secondary chilled water systems in buildings." Energy and Buildings **43**(12): 3646-3656.

Gao, D.; Wang, S.; Sun, Y.; Xiao, F. (2012). "Diagnosis of the low temperature difference syndrome in the chilled water system of a super high-rise building: A case study." Applied Energy **98**: 597-606.

Gordon, J.; Ng, K. (1995). "Predictive and diagnostic aspects of a universal thermodynamic model for chillers." International Journal of Heat and Mass Transfer **38**(5): 807-818.

Gordon, J.; Ng, K. (2000). Cool Thermodynamics: The Engineering and Physics of Predictive, Diagnostic and Optimization Methods for Cooling Systems. Cambridge UK, Cambridge International Science Publishing.

Graves, R. (2003). Thermodynamic modeling and optimization of a screw compressor chiller and cooling tower system. Master of Science, Texas A&M University.

Hattemer, T. (1996). "Chilled water distribution system for an urban university campus." Ashrae **38**(12): 55-57.

Ho, W. F. (1992). "Control strategy: Adjusting chiller outlet water temperature for energy savings." Building Services Engineering Research and Technology **13**(2): 71-78.

Jiang, W.; T Agami Reddy (2003). "Reevaluation of the Gordon-Ng Performance Models for Water-Cooled Chillers." Ashrae Transactions **109**: 272-287.

Sayyar-Rodsari, B.; Smith, A.; Samudra, A. (2013). "Energy-Efficient Operation of a Utility Plant via Predictive Model-Based Optimization Technology." Industrial and Engineering Chemistry Research **53**(13): 5274-5283.

Taylor, S. T. (2002). "Degrading Chilled Water Plant Delta-T: Causes and Mitigation." Ashrae Transactions **108**: 641-653.

Taylor, S. T. (2002). "Primary-Only vs. Primary-Secondary Variable Flow Systems." Ashrae **44**(2): 25-29.

Taylor, S. T. (2011). "Optimizing Design & Control of Chilled Water Plants Part 1: Chilled Water Distribution System Selection." Ashrae **53**(7): 14-25.

Taylor, S. T. (2011). "Optimizing design & control of chilled water plants, part 3: Pipe sizing and optimizing Δt." Ashrae **53**(12): 22-34.

Taylor, S. T. (2011). "Optimizing design & control of chilled water plants: Part 2: Condenser water system design." Ashrae **53**(9): 26-36.

Taylor, S. T. (2012). "Optimizing Design & Control Of Chilled Water Plants Part 5: Optimized Control Sequences." Ashrae **54**(6): 56-74.

Taylor, S. T. (2012). "Optimizing design & control of chilled water plants: Part 4: Chiller & cooling tower selection." Ashrae **54**(3): 60-66.

Wang, G.; Zheng, B.; Liu, M. (2006). Impacts on building return water temperature in district cooling systems. International Solar Energy Conference, Denver, Colorado, 441-448.

Wang, L.; Watt, J.; Zhao, J. (2012). Model Based Building Chilled Water Loop Delta-T Fault Diagnosis. International Conference for Enhanced Building Operations, Manchester, UK.

Wang, Z.; Wang, G.; Xu, K.; Yu, Y.; Liu, M. (2007). Achieving high chilled water delta T without Blending Stations. International Conference for Enhanced Building Operations, San Francisco, California.

Zhang, Z. (2010). Methodology for determining the optimal operating strategies for a chilled water storage system. Doctor of Philosophy, Texas A&M University.

Zhang, Z.; Li, H.; Liu, J. (2012). "Simulations of Chilled Water Cooling Coil Delta-T Characteristics." Ashrae Transactions **118**(2): 349-356.

Zhang, Z.; Turner, W. (2012). Method for Estimating Energy Savings Potential of Chilled-Water Plant Retro-Commissioning Ashrae Transactions.

Zhang, Z. ; Turner, W. ; Chen, Q ; Xu, C ; Deng, S (2011). " Methodology for determining the optimal operating strategies for a chilled-water-storage system-Part I: Theoretical model." Hvac&r Research **17**(5): 737-751.

Zhang, Z. ;Turner, W.; Chen, Q ; Xu, C ; Deng, S (2011). "Methodology for determining the optimal operating strategies for a chilled-water-storage system-Part II: Project application." Hvac&r Research **17**(5): 752-770.

APPENDIX A

The enclosed files contain the data, data analysis, models and final results used in this thesis. The following is a description of the content of each file:

- Plant chilled water data.xlsx
    - DFW Airport chilled water plant hourly data for the period of 6/1/2012 to 5/31/2013.
    - Relevant data includes plant flow and chilled water supply and return temperatures.
    - The file includes the following plots:
        - Delta-T vs load
        - Delta-T vs date
        - ChWST vs date
        - Flow vs load
        - Load vs OAT
        - ChWST vs OAT
- Plant chilled water – monthly analysis.xlsx
    - Plots of the ChWST for each month of data.
- Plant condenser raw data.xlsx
    - Includes condenser water flow and supply and return temperature for each of the chillers.

- TESdata – daily analysis.xlsx
    - Thermal energy storage tank hourly data for the water tank temperature every 2 feet for the height of the tank and water flow rate being discharged from the tank.
    - Primary loop chilled water flow rate, supply and return temperatures.
    - Plots describing tank behavior for one day each month.
- Chiller model.xlsx
    - Individual chiller data for the period from 1/1/2013 to 12/31/2013 that includes:
        - Power
        - Chilled water supply and return temperature
        - Chilled water flow rate
        - Condenser water supply and return temperature
        - Condenser water flow rate
    - Chiller simulation based on the Gordon and Ng model. The file contains the linear regression constants for each chiller.
    - The following plots for each working chiller:
        - Predicted, measured and residual power vs percent load
        - Predicted, measured and residual kW/ton vs percent load
        - Predicted, measured and residual COP vs percent load
        - Predicted vs measured power

- Cooling tower.xlsx
    - Individual chiller data for the period from 1/1/2013 to 12/31/2013 that includes:
        - Power
        - Chilled water supply and return temperature
        - Chilled water flow rate
        - Condenser water supply and return temperature
        - Condenser water flow rate
    - Approach temperature.
    - Plots for the approach temperature and CWST vs Outside air wet bulb temperature for current operation and proposed schedule.
- Chiller model – CWST mod.xlsx
    - Total predicted chiller savings resulting from modifying the CWST to the proposed schedule. The ChWST and condenser water flow rate are maintained as current operation.
- Chiller model – CW flow mod.xlsx
    - Total predicted chiller savings resulting from modifying the condenser water flow rate to the proposed set point. The ChWST and CWST are maintained as current operation.

- Chiller model – ChWST mod.xlsx
    - Total predicted chiller savings resulting from modifying the ChWST to the proposed schedule. The CWST and condenser water flow rate are maintained as current operation.
- Plant second loop dT model.xlsx
    - Linear regression model that simulates the secondary loop delta-T.
    - The file includes the following plots:
        - Measured and predicted delta-T vs load
        - Measured and predicted delta-T vs flow
- TEStank behavior.xlsm – this file includes VBA code.
    - Simulation of the chilled water ratio in the TES tank for different conditions.
    - Predicted net savings for the proposed schedule of ChWST and CWST, maintaining current operation condenser flow rate.
    - Predicted savings for the proposed schedule of ChWST and CWST and proposed condenser flow rate.
- Matlab files
    - Includes all the MATLAB codes used to determine the conditions that yielded the least energy consumption for the chillers.

APPENDIX B

Monthly bill of the central plant

Meter	Type	Dates	Current Meter Read	Previous Meter Read	Multiplier	kWh Usage	kW Demand	Power Factor
004452563WE	ACT	07/25 - 08/24	55966.6	53764.2	720	1,585,703.52		0.857
004452565WE	ACT	07/25 - 08/24	14497.5	11887.1	720	1,893,857.76	18,841.00	0.857
004452564WE	ACT	07/25 - 08/24	19308.6	16302.2	720	2,164,608.00		0.857
004452566WE	ACT	07/25 - 08/24	6994.85	372.664	720	4,767,975.36		0.857

	Qty	Rate	Amount
Current Charges			
Champion Energy Charges			
CKWH : Commercial Energy	10,412,144.64	0.04318	$449,596.41
TDU Delivery Charges			$84,519.48
BAS001:Basic Customer Charge	*1.00*	*14.95000*	*$14.95*
BAS003:Delivery Point Charge	*1.00*	*24.69000*	*$24.69*
DIS001:Distribution Charge	*20,885.00*	*3.37000*	*$70,382.45*
MSC054:Rate Case Expenses Surcharge 2	*20,885.00*	*0.00617*	*$128.78*
TRN002:Firm Point to Point Transmission Service Charge for long term or short term firm	*4,200.00*	*3.32586*	*$13,968.61*
TDU Delivery Charges Non Taxable			$8,855.25
MSC025:Nuclear Decommissioning	*20,885.00*	*0.04500*	*$939.83*
MSC029:Recovery of securitzed portion of stranded assets and costs	*20,885.00*	*0.15400*	*$3,216.29*
MSC036:Recovery of securitized regulatory assets - stranded costs (TC2)	*20,885.00*	*0.22500*	*$4,699.13*
TDU Surcharges			$6,938.82
MSC041:Energy Efficiency Cost Recovery Factor (EECRF)	*10,412,143.00*	*0.00065*	*$6,757.48*
MSC049:Rate Case Expenses Surcharge	*20,885.00*	*0.00868*	*$181.34*
Taxes			
Gross Receipts Reimb			$10,804.86
PUC Assessment			$901.94
Total Current Charges			**$561,616.76**

4CP Demand + PF Adjustment

(3789 KW x 95%) / 85.7% = 4,200 KW

20,885 KW x $3.32586 = $69,461

$55,492 Monthly Savings

$665,904 Annual Savings

+-